Walter+Eliza Hall
Institute of Medical Research

Research Publication Repository

http://publications.wehi.edu.au/search/SearchPublications

This is the author's peer reviewed manuscript version of a work accepted for publication.

Publication details:	Merino D, Whittle JR, Vaillant F, Serrano A, Gong JN, Giner G, Maragno AL, Chanrion M, Schneider E, Pal B, Li X, Dewson G, Grasel J, Liu K, Lalaoui N, Segal D, Herold MJ, Huang DCS, Smyth GK, Geneste O, Lessene G, Visvader JE, Lindeman GJ. Synergistic action of the MCL-1 inhibitor S63845 with current therapies in preclinical models of triple-negative and HER2-amplified breast cancer. Science Translational Medicine. 2017 9(401):eaam7049
Published version is available at:	https://doi.org/10.1126/scitranslmed.aam7049

Changes introduced as a result of publishing processes such as copy-editing and formatting may not be reflected in this manuscript.

Copyright © 2017, American Association for the Advancement of Science

RESEARCH ARTICLE

Synergistic action of the MCL-1 inhibitor S63845 with current therapies in preclinical models of triple negative and HER2-amplified breast cancer

Delphine Merino,[1,2*] James R. Whittle,[1,2,3*] François Vaillant,[1,2*] Antonin Serrano,[1,2] Jia-Nan Gong,[2,4] Goknur Giner,[2,5] Ana Leticia Maragno,[6] Maïa Chanrion,[6] Emilie Schneider,[6] Bhupinder Pal,[1,2] Xiang Li,[2,7] Grant Dewson,[2,7] Julius Gräsel,[1,2] Kevin Liu,[1,2] Najoua Lalaoui,[2,7] David Segal,[2,4] Marco J. Herold,[2,8] David C.S. Huang,[2,4] Gordon K. Smyth,[5,9] Olivier Geneste,[6] Guillaume Lessene,[2,10,11] Jane E. Visvader,[1,2†] Geoffrey J. Lindeman[1,3,12,13†]

[1]ACRF Stem Cells and Cancer Division, The Walter and Eliza Hall Institute of Medical Research, Parkville, VIC 3052, Australia. [2]Department of Medical Biology, The University of Melbourne, Parkville, VIC 3010, Australia. [3]Department of Medical Oncology, The Peter MacCallum Cancer Centre, Melbourne, VIC 3000, Australia. [4]Cancer & Haematology Division, The Walter and Eliza Hall Institute of Medical Research, Parkville, VIC 3052, Australia. [5]Bioinformatics Division, The Walter and Eliza Hall Institute of Medical Research, Parkville, VIC 3052, Australia. [6]Institut de Recherches Servier Oncology R&D Unit, Croissy Sur Seine 78290, France. [7]Cell Signalling & Cell Death Division, The Walter and Eliza Hall Institute of Medical Research, Parkville, VIC 3052, Australia. [8]Molecular Genetics of Cancer Division, The Walter and Eliza Hall Institute of Medical Research, Parkville, VIC 3052, Australia. [9]Department of Mathematics and Statistics, The University of Melbourne, Parkville, VIC 3010, Australia. [10]Chemical Biology Division, The Walter and Eliza Hall Institute of Medical Research, Parkville, VIC 3052, Australia. [11]Department of Pharmacology and Therapeutics, The University of Melbourne, Parkville, VIC 3010, Australia. [12]Department of Medicine, The University of Melbourne, Parkville, VIC 3010, Australia. [13]Parkville Familial Cancer Centre, The Royal Melbourne Hospital and Peter MacCallum Cancer Centre, Parkville, VIC 3050, Australia

*These authors contributed equally to this work

†Corresponding authors. Email: visvader@wehi.edu.au (J.E.V.), lindeman@wehi.edu.au (G.J.L.)

AUTHOR MANUSCRIPT

SUMMARY: The MCL-1 inhibitor S63845 is effective in combination with conventional therapy for targeting triple negative and HER2-amplified breast cancer.

ABSTRACT

The development of BH3 mimetics, which antagonize pro-survival proteins of the BCL-2 family, represents a potential breakthrough in cancer therapy. Targeting the pro-survival member MCL-1 has been an area of intense interest because it is frequently deregulated in cancer. In breast cancer, MCL-1 is often amplified, and high expression predicts poor patient outcome. Here we tested the MCL-1 inhibitor S63845 in breast cancer cell lines and patient-derived xenografts (PDXs) with high expression of MCL-1. S63845 displayed synergistic activity with docetaxel in triple negative breast cancer and with trastuzumab or lapatinib in HER2-amplified breast cancer. Using S63845-resistant cells combined with CRISPR-Cas9 technology, we identified deletion of BAK or upregulation of pro-survival proteins as potential mechanisms that confer resistance to S63845 in breast cancer. Collectively, our findings provide a strong rationale for the clinical evaluation of MCL-1 inhibitors in breast cancer.

INTRODUCTION

Breast cancer is a heterogeneous disease and can be stratified into at least six subgroups based on gene expression profiling: Luminal A, Luminal B (estrogen positive, ER^+), HER2-amplified, basal-like (predominantly triple negative breast cancer, TNBC), claudin-low, and normal-like (*1, 2*). These subtypes predict clinical behavior with respect to response and resistance to therapy, patterns of metastasis, and overall survival. Multiple mechanisms contribute to tumor progression and resistance to cancer therapy, including the evasion of cell death. Cancer cells escape apoptosis through diverse strategies that include increased expression of pro-survival proteins such as BCL-2, BCL-XL, or MCL-1. Targeting these proteins with 'BH3 mimetics' that mimic the function of pro-apoptotic proteins has emerged as a promising strategy in cancer therapy.

The first 'on-target' BH3 mimetic, ABT-737, and its orally bioavailable counterpart ABT-263 (navitoclax), exhibit broad-spectrum activity and inhibit BCL-2, BCL-XL, and BCL-W but not MCL-1 or A1. Clinical application, however, has been hampered by thrombocytopenia induced through concomitant on-target inhibition of BCL-XL in platelets (*3, 4*). The potent BCL-2-specific inhibitor ABT-199 (venetoclax) is platelet-sparing and has demonstrated clinical efficacy as a single agent in the treatment of chronic lymphocytic leukemia (CLL) (*5, 6*). Although navitoclax and venetoclax have single agent activity in some hematologic malignancies, combination therapy strategies are likely to be required for other cancer types (*7*).

In breast cancer, differential expression of pro-survival proteins across tumor subtypes suggests that different members of this protein class could be targeted in distinct tumor subtypes (*8*). *BCL-2*, which is an estrogen-responsive gene, is overexpressed in approximately 85% of ER-positive breast cancer (*9*). In pre-clinical models of luminal B (ER^+) breast cancer, ABT-199 was found to synergize with tamoxifen (*10*), resulting in the evaluation of this combination in the clinic (ISRCTN98335443). MCL-1 may also be a therapeutic target because MCL-1 amplification has been observed in a large-scale high-resolution study of somatic copy-number alterations (SCNAs) across diverse cancers, including breast cancer (*11*), and MCL-1 can confer resistance to chemotherapy or targeted therapy (*12-14*). MCL-1 may promote metastasis (*15*), and high expression has been correlated with poor prognosis (*16*). MCL-1 appears to be the main pro-

AUTHOR MANUSCRIPT

survival protein that is upregulated in TNBC (*17, 18*) and in HER2-amplified tumors, where it may stabilize HER2 and limit the efficacy of HER2-targeted therapies (*19-21*). Moreover, MCL-1 amplification was commonly observed in TNBC tumors that failed to achieve a complete pathological response with neoadjuvant chemotherapy (*22*).

The development of small molecule inhibitors directed against MCL-1 has proved challenging because MCL-1 has a BH3-binding hydrophobic groove that is more rigid than in BCL-XL or BCL-2 (*23*). A number of MCL-1 inhibitors have been recently reported and their activity investigated in vitro, although their potency in vivo is less clear (*18, 24-28*). Recently, a small molecule MCL-1 inhibitor, S63845, which specifically binds with high affinity to the BH3-binding groove of MCL-1, has been developed (*29*). Although S63845 had single agent activity in certain hematopoietic tumor cells, its activity in solid tumors is unclear. As for venetoclax, it is likely that combination therapy will be required (*7, 30*). Here we identify MCL-1 as a potential target in pre-clinical models of TNBC and HER2-amplified breast cancer and demonstrate that S63845 enhances the action of conventional therapy in these breast cancer subtypes.

RESULTS

MCL-1 expression is prominent in TNBC and HER2-amplified tumors

To examine the expression of MCL-1 and other BCL-2 family members across the different subtypes of breast cancer, we first quantified RNA and protein in a cohort of patient derived xenograft (PDX) models (Fig. 1, A and B, fig. S1 and S2, table S1-3). As previously reported (*9, 10*), *BCL-2* mRNA and protein were most highly expressed in ER^+ breast cancer. Conversely, *MCL-1* expression was higher in TNBC (including *BRCA1*-mutated tumors) and HER2-amplified tumors, compared to ER-positive tumors. Similar findings were observed in primary breast tumors from the METABRIC or TCGA datasets (fig. S3, A and B, table S4) (*1, 31*). In agreement with RNA expression, the highest amount of MCL-1 protein was observed in TNBC PDXs, although MCL-1 was expressed across the entire repertoire of PDX tumors. BCL-XL protein was present in high amounts across all tumors, despite apparently higher mRNA expression in the HER2-amplified subset. The amounts of transcript of another pro-survival family member, *BCL-W*, were similar across subtypes and present at low levels. The key BH3-only pro-apoptotic protein, BIM, was generally expressed in lower amounts in TNBC compared

to ER-positive PDXs. BCL-2 family protein expression was confirmed by immunohistochemistry in two TNBC PDX models (838 and 110) and one HER2-amplified PDX model (231) (fig. S4, A and B).

The potency of the MCL-1 specific inhibitor S63845 as an inducer of cell death was first tested in a panel of six breast cancer cell lines, which expressed MCL-1 (Fig. 1C and D). The response varied across cell lines, consistent with recent findings for other cancer types (*29*) and for the MCL-1 inhibitor A-1210477 (*18*) or MCL-1-specific siRNAs (*17*). The HER2-amplified cell line SK-BR-3 was most sensitive to S63845, followed by the TNBC cell lines, BT-20 and MDA-MB-468. In contrast, the ER-positive MCF-7 and BT-474 cell lines as well as the claudin-low TNBC MDA-MB-231 cell line were more resistant. It is possible that differences in BCL-XL and BCL-2 expression in these cell lines (Fig. 1D) account for their differential response. For example, SK-BR-3 cells have low expression of BCL-2 and high expression of BAK, which could have contributed to their increased sensitivity to S63845 compared to the other cell lines.

We next studied the sensitivity of three HER2-amplified and five TNBC PDX models to the BH3 mimetics ABT-737, ABT-199, WEHI-539 (a BCL-XL inhibitor) (*32*), and S63845 in short-term culture assays. In contrast to other BH3 mimetics, all tumors displayed sensitivity to 1 μM S63845, most notably the TNBC models (Fig. 1E, fig. S1C). The IC50 for most PDX models was less than 1 μM for most models (except for PDX 951 and 45). These findings suggest that MCL-1 is an important survival factor in TNBC and HER2-amplified subtypes. Both *BRCA1*-mutated (303, 110) and wild-type (838, 322, and 744) TNBC PDXs, which had similar MCL-1 expression, were sensitive to S63845 (Fig. 1E). S63845 appeared to be a more effective inducer of cell death than the MCL-1 compound A-1210477 in SK-BR-3 cells (fig. S1C and D), consistent with its reported potency (*29*). Together these findings suggest that MCL-1 could be an important survival factor and therapeutic target in TNBC and HER2-amplified tumors.

S63845 activity is dependent on BAK and is curtailed by pro-survival family members

To explore mechanisms that underpin tumor response or resistance to S63845, we performed a genome-wide CRISPR-Cas9 screen in SK-BR-3 cells, which were highly sensitive to this agent. SK-BR-3 Cas9 expressing cells were transduced with a pooled human genome-wide gRNA

AUTHOR MANUSCRIPT

lentiviral library containing 123,411 unique sgRNAs targeting 19,050 genes and 1,864 miRNAs (6 sgRNAs per gene and 4 sgRNAs per miRNA) at low multiplicity of infection (MOI) in six independent infections (*33*). Next generation sequencing (NGS) of the transduced cells confirmed high representation of the sgRNA library. Most (96%) of the library sgRNAs were present, with 6 sgRNAs detected for 79% of genes (fig. S5A). Each transduced cell line was treated with either S63845 (1 μM) or DMSO (control), and genomic DNA of the surviving cells was subsequently isolated and sgRNAs identified by NGS. As expected, the number of sgRNAs was reduced in the S63845 treated groups, indicating high selective pressure from S63845. This resulted in a high Gini index, denoting reduced complexity of the represented sgRNAs in the S63845 treated groups when compared to DMSO treated controls (fig. S5B). *BAK* emerged as a key mediator of resistance, because it was the only gene for which more than one sgRNA was detected in the resistant cell clones in all replicates (Fig. 2A, table S5). This finding is consistent with those reported for A-1210477 (*18*) and suggests that S63845 likely kills through disruption of MCL-1/BAK complexes or by preventing sequestration of BAK by MCL-1 (*34*).

To further investigate the role of BCL-2 family members, we performed a focused CRISPR-Cas9 screen targeting the pro-apoptotic BCL-2 family members (Fig. 2B, fig. S5C, tables S6 and S7). Cells were transduced with lentiviruses expressing sgRNAs that targeted various pro-apoptotic genes, and then treated with increasing concentrations of S63845. Consistent with the genome-wide screen, only sgRNAs targeting *BAK* conferred resistance to apoptosis in SK-BR-3 cells treated with the MCL-1 inhibitor. Although targeting *BAX* alone did not confer resistance, *BAX/BAK* double-knockout cells were completely resistant to S63845. The dependency on BAK and BAX confirms that this small molecule inhibitor specifically targets the intrinsic (BCL-2 family) apoptotic pathway (fig. S5D). Targeting of single BH3-only genes did not confer resistance to S63845 (Fig. 2B).

To confirm that S63845 can disrupt complexes containing MCL-1 and BH3 only proteins, we performed co-immunoprecipitation studies where HEK293T cells were transfected with a FLAG-tagged MCL-1 construct and HA- or EE-tagged BH3 proteins and cultured in the presence or absence of S63845. After immunoprecipitation of FLAG-tagged MCL-1, co-immunoprecipitated HA- or EE-tagged proteins were identified by western blot analysis. As

expected from the CRISP-Cas9 knockdown studies (Fig. 2, A and B), disruption of MCL-1/BAK complexes was readily detected (fig. S5E). In addition, we found that S63845 disrupted other MCL-1 complexes containing BIM, PUMA, BID, NOXA, or BMF (fig. S5E). Together, these findings reveal the potential importance of S63845 in disrupting MCL-1 complexes containing several BH3 sensor proteins. Because deletion of a single BH3-only protein did not affect sensitivity to S63845 (Fig. 2B), these findings suggest some level of functional redundancy between MCL-1 interacting proteins. To test this hypothesis, we generated SK-BR-3 cells deficient in BIM/BID and BIM/BID/PUMA (fig. S5F). Targeting both *BIM* and *BID* induced only a partial resistance to S63845, whereas concurrent targeting of *BIM, BID,* and *PUMA* greatly impaired S63845-mediated cell death (Fig. 2C), indicating that these BH3-only proteins exert a redundant function in these cells.

We next generated a model of acquired resistance by continuous treatment of BT-20, MDA-MB-468, and BT-474 cell lines with S63845 at either 200 nM or 1 μM for six weeks (fig. S6A), and confirmed resistance by retreatment with S63845 (fig. S6B). S63845 resistant MDA-MB-468 cells were more sensitive to BCL-2 and BCL-XL inhibition than treatment-naïve cells, suggesting that concurrent targeting of other pro-survival proteins may help to trigger a response in some tumors. In keeping with this notion, the sensitivity of MDA-MB-468 and MDA-MB-231 cells to S63845 was increased by concomitant treatment with ABT-737, and to a lesser extent by WEHI-539 or ABT-199 (Fig. 2D and fig. S7A). In contrast, BT-474 and MDA-MB-468 resistant clones failed to be sensitized to BCL-2 and BCL-XL inhibition, despite resistant BT-474 cells containing more BCL-2 (fig. S6A). This observation suggests that other mechanisms of resistance may have an important role in these cell lines. Because most resistant clones exhibited lower amounts of BIM and BAK (fig. S6B), reduced expression of these pro-apoptotic proteins could have contributed to acquired resistance. In addition, overexpression of MCL-1 in SK-BR-3 cells reduced the potency of the inhibitor (fig. S7, B and C), indicating that enforced expression of MCL-1 can also modulate response to S63845.

To further explore the relative contribution of other pro-survival proteins to the survival of breast cancer cells in models of innate resistance, we examined the activity of different BH3 mimetics combined with S63845 in two S63845-sensitive PDX models (303 and 838) and two less

AUTHOR MANUSCRIPT

sensitive models (45 and 951) (Fig. 2E). The combination of S63845 with ABT-737 or WEHI-539 enhanced the killing of tumor cells, indicating that these cells depended on both MCL-1 and BCL-XL for survival. Addition of the BCL-2 inhibitor ABT-199 to S63845 was moderately effective in killing 951 and 303 PDX cells but had no effect on 45 PDX cells, consistent with its low BCL-2 expression (fig. S1B). This PDX model was intrinsically resistant to MCL-1 (S63845, IC50 >1 μM), even though BAK was localized to the mitochondria and appeared to be functional in mitochondrial assays (fig. S7D). Thus, the relative resistance of the 45 and 951 PDX models to S63845-induced cell death is likely to be mediated by BCL-XL and/or BCL-2.

Taken together, these findings indicate that loss of BAK or augmented expression of other pro-survival proteins, particularly BCL-XL, are likely to be the main factors with potential to produce resistance to S63845 in TNBC and HER2-overexpressing breast cancer cells. Therefore, maximal induction of apoptosis could be achieved by targeting additional pro-survival proteins, or through concomitant therapy that primes cells for apoptosis.

S63845 synergizes with docetaxel, lapatinib, or trastuzumab in vitro

MCL-1 inhibitors are most likely to be effective in breast cancer therapy when used in conjunction with a 'priming' agent that delivers another apoptotic signal. We therefore investigated whether S63845 elicited synergistic activity with agents currently used in the treatment of TNBC and HER2-amplified breast cancer. SK-BR-3 cells were treated with S63845 combined with the dual receptor tyrosine kinase inhibitor lapatinib, the anti-HER2 monoclonal antibody trastuzumab, or the taxane docetaxel (Fig. 3A). Docetaxel and S63845 elicited marked synergy at very low concentrations of docetaxel (2 nM) and S63845 (30 nM) (Fig. 3, A and B). Similarly, S63845 synergy was observed with both lapatinib and trastuzumab (Fig. 3, A and C), although slightly longer cotreatment was required for trastuzumab, presumably due to its different mechanism of action. Inhibition of caspases with Q-VD-OPh efficiently blocked cell death, confirming that cell death was via apoptosis (Fig. 3, A and D).

We next compared S63845 to other BH3 mimetics as inducers of apoptosis alone or in combination with trastuzumab, docetaxel, or lapatinib (fig. S8). SK-BR-3 cells were treated with increasing concentrations of S63845, ABT-737, ABT-199, or WEHI-539 (up to 2 μM) in the

presence of vehicle, trastuzumab, lapatinib, or docetaxel. Treatment provoked cell death that was markedly augmented when combined with S63845 but not the other BH3 mimetics (fig. S8, A-D), consistent with the synergy observed above between S63845 and conventional therapy.

Although BCL-XL has been reported to be down-regulated after lapatinib treatment (*35*), the amount of BCL-XL did not appreciably change at the low doses deployed here (Fig. 3D), and BCL-2 was undetectable in this cell line (Fig. 1D). The amounts of BID, which contributed to S63845-mediated sensitivity (Fig. 2C), were also similar after treatment with the various agents. Moreover, knockdown of *BID* using CRISPR-Cas9-mediated editing revealed that BID was not required for the synergistic effect of S63845 with docetaxel or anti-HER2 therapy (fig. S9A). In contrast, BIM protein expression increased after lapatinib treatment (Fig. 3D). This was presumably due to decreased AKT and ERK activation (P-ERK and P-AKT), which phosphorylates BIM and thereby reduces BIM levels (*29*). To explore a potential role for BIM in the synergistic response, we treated BIM-deficient clones (achieved through CRISPR-Cas9-mediated editing of *BIM*) with S63845 plus trastuzumab, lapatinib, or docetaxel (fig. S9A). Although *BIM* deletion did not completely block the cytotoxic activity of any of these drugs, it significantly reduced their synergy at low concentrations ($p<0.05$). These results are consistent with a previous study showing the potential contribution of the BIM/MCL-1 complexes in HER2-overexpressing breast cancer cells (*36*). We further confirmed that S63845 was able to disrupt BIM/MCL-1 complexes in PDX derived cells (fig. S9B). Taken together, these findings suggest a key role for BIM in the synergistic action of S63845 with docetaxel or anti-HER2 therapy.

AUTHOR MANUSCRIPT

MCL-1 inhibition sensitizes PDX tumors to conventional therapy in vivo

Because in vitro assays revealed that both breast cancer cell lines and PDX-derived cells were sensitive to S63845 in combination therapy, we next determined their therapeutic effect in vivo using PDX models, including two TNBC and one HER2-amplified model (Fig. 4, fig. S10). S63845 alone was insufficient to inhibit tumor growth. Nonetheless, S63845 synergized with docetaxel or trastuzumab, resulting in improved survival. For the 110 and 838 PDX models, mice were treated with docetaxel (every three weeks) and S63845 (weekly) for two treatment cycles (Fig. 4, A and B, fig. S10). Tumor growth was impeded by combination therapy, although

tumors relapsed after treatment was stopped. Evaluation of tumor lysates from mice bearing PDX 838 tumors after short term treatment revealed increased cleaved caspase 3 after combination therapy, consistent with augmented tumor cell death (fig. S11A and B). The addition of S63845 to twice weekly trastuzumab also augmented responsiveness in the HER2-amplified 231 PDX model (Fig. 4C). Notably, S63845 therapy appeared to be well tolerated in combination therapy with either docetaxel or trastuzumab, with mice maintaining normal body weight during therapy (fig. S12A). No perturbation in urea, creatinine and liver enzymes (fig. S12B), or blood counts (fig. S12C) was observed after S63845 treatment. These results suggest that combining MCL-1 inhibitors with either chemotherapy or HER2-targeted therapy has the potential to enhance tumor response and clinical outcome.

DISCUSSION

MCL-1 is a crucial regulator of cell survival in both normal and neoplastic cells and is often responsible for resistance to anti-cancer therapy (*37-39*). The observation that MCL-1 is amplified in breast cancer (*11*), together with recent reports indicating that breast cancer cells depend on MCL-1 for survival, suggest a potential clinical role for MCL-1 inhibitors (*17, 18*). In this study, we tested the MCL-1 inhibitor S63845 in breast cancer cell lines and PDX tumor cells in vitro and observed synergistic activity with docetaxel in TNBC and with trastuzumab in HER2-amplified tumor cells. This synergy translated into improved tumor response in vivo and enhanced overall survival in PDX models. Given that Fc Receptor-mediated cell death is lacking in NSG mice, it is possible that a more profound effect of anti-HER2 monoclonal antibody therapy might be observed in immunocompetent models and patients.

We previously demonstrated that inhibition of BCL-2 and BCL-XL with ABT-737 alone was insufficient to inhibit the growth of TNBC tumors (*40*). Although PDX tumor cells appeared to be more sensitive to S63845 than to BCL-2- or BCL-XL-specific inhibitors in vitro, S63845 alone did not induce a clinical response in TNBC and HER2-amplified PDX tumors. It is possible that a lower IC50, similar to that recently described for leukemic cells (*29*), is required to elicit an in vivo tumor response to single agent therapy. Moreover, since the addition of other BH3 mimetics greatly enhanced the efficacy of S63845, TNBC and HER2-amplified breast

cancer cells likely deploy additional pro-survival BCL-2 family members, in contrast to certain leukemic cell types where a single pro-survival protein can have a dominant role (*41*).

S63845 notably attenuated tumor growth in combination with docetaxel in TNBC and trastuzumab in HER2-amplified PDX models. Both docetaxel and trastuzumab have been shown to reduce MCL-1 (*20, 35, 42*), perhaps in part accounting for the augmented response to combination therapy, although MCL-1 expression did not appear to be modulated at the doses used here. Synergism between docetaxel and ABT-737 or the BCL-XL inhibitor A-1331852 has also been observed (*40, 42, 43*), suggesting that direct inhibition of BCL-XL and MCL-1 with BH3-mimetics could be investigated. Indeed, dual treatment of cell lines with the BCL-XL inhibitor WEHI-539 and the MCL-1 inhibitor A-1210477 in vitro appears to be efficacious and may sensitize cells to chemotherapy (*44*). It remains to be established, however, whether there is a suitable therapeutic window for combining the potent MCL-1 inhibitor S63845 with other BH3-mimetics in vivo.

Despite the observation that MCL-1 deletion is lethal in knockout mice (*45*) and previous reports pointing to a crucial physiological role for MCL-1 in many cell types including cardiomyocytes (*46, 47*), we found that the administration of S63845 was well-tolerated, in agreement with a recent report (*29*). This may be due to partial inhibition of MCL-1 in the adult rather than complete deletion during critical developmental time points. In addition, the selectivity of the compound in cancer cells at the doses used in our pre-clinical models may be explained through tumor 'priming' (*41*), or through the drug's greater binding affinity for human compared to mouse MCL-1. Finally, MCL-1 also plays an important role in mitochondrial respiration (*48*). S63845 may not interfere with this function because BH3-mimetics compete for binding to the hydrophobic groove, a conformational pocket on the surface of pro-survival proteins that is specifically involved in binding BH3-only proteins (*49*). It will be important to investigate the safety of MCL-1 inhibitors and combination therapy in the clinic.

Innate and acquired resistance to therapy remains a major challenge for patients with breast cancer. Our results predict that loss of BAK may be a potential mechanism of acquired resistance to S63845-induced cell death. Sequestration of BAK by MCL-1 might represent the primary

AUTHOR MANUSCRIPT

anti-apoptotic function in these cells. This mechanism has been described as 'Mode 2' in the unified model (*50*). It is also possible that BH3-only proteins (sensitizers and/or activators) are required after S63845 treatment ('Mode 1'). Our results using BIM/PUMA/BID-deficient SK-BR-3 cells support this latter model, because these BH3-only proteins were required for BAX/BAK activation in this cell line. It is noteworthy, however, that the CRISPR-Cas9 screen did not identify any single BH3-only protein directly involved in S63845-mediated cell death, despite the ability of the compound to displace most BH3-only proteins from MCL-1. These results suggest a great degree of functional redundancy amongst BH3-only proteins in breast cancer. However, BIM deletion partially impaired the synergistic effect of S63845 with docetaxel, lapatinib, and trastuzumab. In addition, the prolonged inhibition of MCL-1 can cause the up-regulation of other pro-survival proteins, similar to that seen in the case of an ABT-737-mediated increase in MCL-1 (*51, 52*). Cumulatively, our findings suggest that either BAK inactivation or upregulation of pro-survival proteins represent possible strategies that could be deployed by tumor cells to acquire resistance to prolonged therapy.

The recent development of the potent MCL-1 inhibitor S63845 has boosted the prospects of targeting tumor cell dependence on this key pro-survival factor. Indeed, a counterpart clinical lead compound S64315 is now under investigation in human studies (Clinicaltrial.gov Identifier NCT02992483). Here we identify MCL-1 as an important target in TNBC and HER2-amplified breast cancer and further demonstrate that S63845 is an on-target MCL-1 inhibitor with promising activity using patient-derived xenograft models. These findings provide a strong rationale for its further investigation in the clinic.

MATERIALS AND METHODS

Study design

The study was designed to evaluate the response of breast cancer cells to the MCL-1 inhibitor S63845. We evaluated the response to S63845 alone or in combination with conventional therapy (docetaxel or anti-HER2 therapies) in triple negative and HER2-amplified cell lines in vitro and PDX tumor models in vivo. Experiments were designed to investigate the mechanisms

of tumor response. As outlined below, all mouse studies included randomization and blinding. The numbers of replicates performed for each experiment are included in the figure legends.

Statistical Analysis

All statistical tests were two-sided. For the in vivo tumor studies, statistical analyses were performed in the GraphPad Prism software version 5.0a. Kaplan-Meier (log rank test) was used to test for significant differences in the survival of mice (using the ethical end point for tumor size as a surrogate for death). Unpaired t tests were used to test the significance of differences in column means between treatments.

AUTHOR MANUSCRIPT

SUPPLEMENTARY MATERIALS

Materials and Methods

References (10, 33, 40, 53-66)

Fig. S1. Expression of BCL-2 family members and sensitivity to S63845 or A-1210477.

Fig. S2. RNAseq analysis of BCL-2 family members in PDX models.

Fig. S3. Expression of *BCL-XL*, *BCL-2*, *BCL-W* and *MCL-1* in METABRIC and TCGA databases.

Fig. S4. Characterization of ER, PR, HER2, and BCL-2 family member protein expression in PDX models by immunohistochemistry.

Fig. S5. Deep sequencing of genome-wide lentiviral sgRNA libraries, knockdown of BH3 proteins and S63845 mediated disruption of MCL-1 complexes containing BH3-only proteins.

Fig. S6 Generation and analysis of S63845 resistant cell lines.

Fig. S7. Exploring molecular mechanisms of resistance to S63845.

Fig. S8. Effect of concomitant treatment of SK-BR-3 cells with a BH3 mimetic and trastuzumab, lapatinib or docetaxel.

Fig. S9. Role of BIM in the synergistic effect of S63845.

Fig. S10. Individual tumor growth curves in TNBC and HER2-amplified PDXs after treatment with S63845 and docetaxel or trastuzumab.

Fig. S11. Effect of combination therapy on tumor cell death.

Fig. S12 Effect of combination therapy on mouse weight, biochemistry and blood counts.

Table S1. Clinical, histopathological and molecular features of primary breast tumors.

Table S2. BCL-2 family mRNA expression in PDX models.

Table S3. Statistical analysis of gene expression between different molecular subtypes of breast cancer in PDX models.

Table S4. Statistical analysis of *MCL-1*, *BCL-2*, *BCL-XL* and *BCL-W* gene expression between different molecular subtypes of breast cancer in METABRIC and TCGA datasets.

Table S5. Normalized sgRNA counts upregulated in S63845 treated cells compared to DMSO control.

Table S6. Primers used for sequencing CRISPR clones.

Table S7. Sequencing analysis of CRISPR clones for *BAK*, *BAX, BMF,* and *NOXA.*

REFERENCES AND NOTES

1. C. Curtis, S. P. Shah, S. F. Chin, G. Turashvili, O. M. Rueda, M. J. Dunning, D. Speed, A. G. Lynch, S. Samarajiwa, Y. Yuan, S. Graf, G. Ha, G. Haffari, A. Bashashati, R. Russell, S. McKinney, M. Group, A. Langerod, A. Green, E. Provenzano, G. Wishart, S. Pinder, P. Watson, F. Markowetz, L. Murphy, I. Ellis, A. Purushotham, A. L. Borresen-Dale, J. D. Brenton, S. Tavare, C. Caldas, S. Aparicio, The genomic and transcriptomic architecture of 2,000 breast tumours reveals novel subgroups. *Nature* **486**, 346-352 (2012).
2. A. Prat, C. M. Perou, Deconstructing the molecular portraits of breast cancer. *Mol Oncol* **5**, 5-23 (2011).
3. K. D. Mason, M. R. Carpinelli, J. I. Fletcher, J. E. Collinge, A. A. Hilton, S. Ellis, P. N. Kelly, P. G. Ekert, D. Metcalf, A. W. Roberts, D. C. Huang, B. T. Kile, Programmed anuclear cell death delimits platelet life span. *Cell* **128**, 1173-1186 (2007).
4. T. Oltersdorf, S. W. Elmore, A. R. Shoemaker, R. C. Armstrong, D. J. Augeri, B. A. Belli, M. Bruncko, T. L. Deckwerth, J. Dinges, P. J. Hajduk, M. K. Joseph, S. Kitada, S. J. Korsmeyer, A. R. Kunzer, A. Letai, C. Li, M. J. Mitten, D. G. Nettesheim, S. Ng, P. M. Nimmer, J. M. O'Connor, A. Oleksijew, A. M. Petros, J. C. Reed, W. Shen, S. K. Tahir, C. B. Thompson, K. J. Tomaselli, B. Wang, M. D. Wendt, H. Zhang, S. W. Fesik, S. H. Rosenberg, An inhibitor of Bcl-2 family proteins induces regression of solid tumours. *Nature* **435**, 677-681 (2005).

5. A. W. Roberts, M. S. Davids, J. M. Pagel, B. S. Kahl, S. D. Puvvada, J. F. Gerecitano, T. J. Kipps, M. A. Anderson, J. R. Brown, L. Gressick, S. Wong, M. Dunbar, M. Zhu, M. B. Desai, E. Cerri, S. Heitner Enschede, R. A. Humerickhouse, W. G. Wierda, J. F. Seymour, Targeting BCL2 with Venetoclax in Relapsed Chronic Lymphocytic Leukemia. *N Engl J Med* **374**, 311-322 (2016).
6. A. J. Souers, J. D. Leverson, E. R. Boghaert, S. L. Ackler, N. D. Catron, J. Chen, B. D. Dayton, H. Ding, S. H. Enschede, W. J. Fairbrother, D. C. Huang, S. G. Hymowitz, S. Jin, S. L. Khaw, P. J. Kovar, L. T. Lam, J. Lee, H. L. Maecker, K. C. Marsh, K. D. Mason, M. J. Mitten, P. M. Nimmer, A. Oleksijew, C. H. Park, C. M. Park, D. C. Phillips, A. W. Roberts, D. Sampath, J. F. Seymour, M. L. Smith, G. M. Sullivan, S. K. Tahir, C. Tse, M. D. Wendt, Y. Xiao, J. C. Xue, H. Zhang, R. A. Humerickhouse, S. H. Rosenberg, S. W. Elmore, ABT-199, a potent and selective BCL-2 inhibitor, achieves antitumor activity while sparing platelets. *Nat Med* **19**, 202-208 (2013).
7. A. W. Roberts, D. Huang, Targeting BCL2 With BH3 Mimetics: Basic Science and Clinical Application of Venetoclax in Chronic Lymphocytic Leukemia and Related B Cell Malignancies. *Clin Pharmacol Ther* **101**, 89-98 (2017).
8. D. Merino, S. W. Lok, J. E. Visvader, G. J. Lindeman, Targeting BCL-2 to enhance vulnerability to therapy in estrogen receptor-positive breast cancer. *Oncogene* **35**, 1877-1887 (2016).
9. S. J. Dawson, N. Makretsov, F. M. Blows, K. E. Driver, E. Provenzano, J. Le Quesne, L. Baglietto, G. Severi, G. G. Giles, C. A. McLean, G. Callagy, A. R. Green, I. Ellis, K. Gelmon, G. Turashvili, S. Leung, S. Aparicio, D. Huntsman, C. Caldas, P. Pharoah, BCL2 in breast cancer: a favourable prognostic marker across molecular subtypes and independent of adjuvant therapy received. *Br J Cancer* **103**, 668-675 (2010).
10. F. Vaillant, D. Merino, L. Lee, K. Breslin, B. Pal, M. E. Ritchie, G. K. Smyth, M. Christie, L. J. Phillipson, C. J. Burns, G. B. Mann, J. E. Visvader, G. J. Lindeman, Targeting BCL-2 with the BH3 mimetic ABT-199 in estrogen receptor-positive breast cancer. *Cancer Cell* **24**, 120-129 (2013).
11. R. Beroukhim, C. H. Mermel, D. Porter, G. Wei, S. Raychaudhuri, J. Donovan, J. Barretina, J. S. Boehm, J. Dobson, M. Urashima, K. T. Mc Henry, R. M. Pinchback, A. H. Ligon, Y. J. Cho, L. Haery, H. Greulich, M. Reich, W. Winckler, M. S. Lawrence, B. A. Weir, K. E.

AUTHOR MANUSCRIPT

Tanaka, D. Y. Chiang, A. J. Bass, A. Loo, C. Hoffman, J. Prensner, T. Liefeld, Q. Gao, D. Yecies, S. Signoretti, E. Maher, F. J. Kaye, H. Sasaki, J. E. Tepper, J. A. Fletcher, J. Tabernero, J. Baselga, M. S. Tsao, F. Demichelis, M. A. Rubin, P. A. Janne, M. J. Daly, C. Nucera, R. L. Levine, B. L. Ebert, S. Gabriel, A. K. Rustgi, C. R. Antonescu, M. Ladanyi, A. Letai, L. A. Garraway, M. Loda, D. G. Beer, L. D. True, A. Okamoto, S. L. Pomeroy, S. Singer, T. R. Golub, E. S. Lander, G. Getz, W. R. Sellers, M. Meyerson, The landscape of somatic copy-number alteration across human cancers. *Nature* **463**, 899-905 (2010).

12. S. H. Wei, K. Dong, F. Lin, X. Wang, B. Li, J. J. Shen, Q. Zhang, R. Wang, H. Z. Zhang, Inducing apoptosis and enhancing chemosensitivity to gemcitabine via RNA interference targeting Mcl-1 gene in pancreatic carcinoma cell. *Cancer Chemother Pharmacol* **62**, 1055-1064 (2008).
13. I. E. Wertz, S. Kusam, C. Lam, T. Okamoto, W. Sandoval, D. J. Anderson, E. Helgason, J. A. Ernst, M. Eby, J. Liu, L. D. Belmont, J. S. Kaminker, K. M. O'Rourke, K. Pujara, P. B. Kohli, A. R. Johnson, M. L. Chiu, J. R. Lill, P. K. Jackson, W. J. Fairbrother, S. Seshagiri, M. J. Ludlam, K. G. Leong, E. C. Dueber, H. Maecker, D. C. Huang, V. M. Dixit, Sensitivity to antitubulin chemotherapeutics is regulated by MCL1 and FBW7. *Nature* **471**, 110-114 (2011).
14. W. J. Placzek, J. Wei, S. Kitada, D. Zhai, J. C. Reed, M. Pellecchia, A survey of the anti-apoptotic Bcl-2 subfamily expression in cancer types provides a platform to predict the efficacy of Bcl-2 antagonists in cancer therapy. *Cell Death Dis* **1**, e40 (2010).
15. A. I. Young, A. M. Law, L. Castillo, S. Chong, H. D. Cullen, M. Koehler, S. Herzog, T. Brummer, E. F. Lee, W. D. Fairlie, M. C. Lucas, D. Herrmann, A. Allam, P. Timpson, D. N. Watkins, E. K. Millar, S. A. O'Toole, D. Gallego-Ortega, C. J. Ormandy, S. R. Oakes, MCL-1 inhibition provides a new way to suppress breast cancer metastasis and increase sensitivity to dasatinib. *Breast Cancer Res* **18**, 125 (2016).
16. Q. Ding, X. He, W. Xia, J. M. Hsu, C. T. Chen, L. Y. Li, D. F. Lee, J. Y. Yang, X. Xie, J. C. Liu, M. C. Hung, Myeloid cell leukemia-1 inversely correlates with glycogen synthase kinase-3beta activity and associates with poor prognosis in human breast cancer. *Cancer Res* **67**, 4564-4571 (2007).

17. C. M. Goodwin, O. W. Rossanese, E. T. Olejniczak, S. W. Fesik, Myeloid cell leukemia-1 is an important apoptotic survival factor in triple-negative breast cancer. *Cell Death Differ* **22**, 2098-2106 (2015).
18. Y. Xiao, P. Nimmer, G. S. Sheppard, M. Bruncko, P. Hessler, X. Lu, L. Roberts-Rapp, W. N. Pappano, S. W. Elmore, A. J. Souers, J. D. Leverson, D. C. Phillips, MCL-1 Is a Key Determinant of Breast Cancer Cell Survival: Validation of MCL-1 Dependency Utilizing a Highly Selective Small Molecule Inhibitor. *Mol Cancer Ther* **14**, 1837-1847 (2015).
19. M. H. Bashari, F. Fan, S. Vallet, M. Sattler, M. Arn, C. Luckner-Minden, H. Schulze-Bergkamen, I. Zornig, F. Marme, A. Schneeweiss, M. H. Cardone, J. T. Opferman, D. Jager, K. Podar, Mcl-1 confers protection of Her2-positive breast cancer cells to hypoxia: therapeutic implications. *Breast Cancer Res* **18**, 26 (2016).
20. E. S. Henson, X. Hu, S. B. Gibson, Herceptin sensitizes ErbB2-overexpressing cells to apoptosis by reducing antiapoptotic Mcl-1 expression. *Clin Cancer Res* **12**, 845-853 (2006).
21. C. Mitchell, A. Yacoub, H. Hossein, A. P. Martin, M. D. Bareford, P. Eulitt, C. Yang, K. P. Nephew, P. Dent, Inhibition of MCL-1 in breast cancer cells promotes cell death in vitro and in vivo. *Cancer Biol Ther* **10**, 903-917 (2010).
22. J. M. Balko, J. M. Giltnane, K. Wang, L. J. Schwarz, C. D. Young, R. S. Cook, P. Owens, M. E. Sanders, M. G. Kuba, V. Sanchez, R. Kurupi, P. D. Moore, J. A. Pinto, F. D. Doimi, H. Gomez, D. Horiuchi, A. Goga, B. D. Lehmann, J. A. Bauer, J. A. Pietenpol, J. S. Ross, G. A. Palmer, R. Yelensky, M. Cronin, V. A. Miller, P. J. Stephens, C. L. Arteaga, Molecular profiling of the residual disease of triple-negative breast cancers after neoadjuvant chemotherapy identifies actionable therapeutic targets. *Cancer Discov* **4**, 232-245 (2014).
23. P. E. Czabotar, E. F. Lee, M. F. van Delft, C. L. Day, B. J. Smith, D. C. Huang, W. D. Fairlie, M. G. Hinds, P. M. Colman, Structural insights into the degradation of Mcl-1 induced by BH3 domains. *Proc Natl Acad Sci U S A* **104**, 6217-6222 (2007).
24. N. A. Cohen, M. L. Stewart, E. Gavathiotis, J. L. Tepper, S. R. Bruekner, B. Koss, J. T. Opferman, L. D. Walensky, A competitive stapled peptide screen identifies a selective small molecule that overcomes MCL-1-dependent leukemia cell survival. *Chem Biol* **19**, 1175-1186 (2012).
25. A. Friberg, D. Vigil, B. Zhao, R. N. Daniels, J. P. Burke, P. M. Garcia-Barrantes, D. Camper, B. A. Chauder, T. Lee, E. T. Olejniczak, S. W. Fesik, Discovery of potent myeloid cell

AUTHOR MANUSCRIPT

leukemia 1 (Mcl-1) inhibitors using fragment-based methods and structure-based design. *J Med Chem* **56**, 15-30 (2013).

26. T. Lee, Z. Bian, B. Zhao, L. J. Hogdal, J. L. Sensintaffar, C. M. Goodwin, J. Belmar, S. Shaw, J. C. Tarr, N. Veerasamy, S. M. Matulis, B. Koss, M. A. Fischer, A. L. Arnold, D. V. Camper, C. F. Browning, O. W. Rossanese, A. Budhraja, J. Opferman, L. H. Boise, M. R. Savona, A. Letai, E. T. Olejniczak, S. W. Fesik, Discovery and biological characterization of potent myeloid cell leukemia-1 inhibitors. *FEBS Lett*, (2016).
27. J. D. Leverson, H. Zhang, J. Chen, S. K. Tahir, D. C. Phillips, J. Xue, P. Nimmer, S. Jin, M. Smith, Y. Xiao, P. Kovar, A. Tanaka, M. Bruncko, G. S. Sheppard, L. Wang, S. Gierke, L. Kategaya, D. J. Anderson, C. Wong, J. Eastham-Anderson, M. J. Ludlam, D. Sampath, W. J. Fairbrother, I. Wertz, S. H. Rosenberg, C. Tse, S. W. Elmore, A. J. Souers, Potent and selective small-molecule MCL-1 inhibitors demonstrate on-target cancer cell killing activity as single agents and in combination with ABT-263 (navitoclax). *Cell Death Dis* **6**, e1590 (2015).
28. M. L. Stewart, E. Fire, A. E. Keating, L. D. Walensky, The MCL-1 BH3 helix is an exclusive MCL-1 inhibitor and apoptosis sensitizer. *Nat Chem Biol* **6**, 595-601 (2010).
29. A. Kotschy, Z. Szlavik, J. Murray, J. Davidson, A. L. Maragno, G. Le Toumelin-Braizat, M. Chanrion, G. L. Kelly, J. N. Gong, D. M. Moujalled, A. Bruno, M. Csekei, A. Paczal, Z. B. Szabo, S. Sipos, G. Radics, A. Proszenyak, B. Balint, L. Ondi, G. Blasko, A. Robertson, A. Surgenor, P. Dokurno, I. Chen, N. Matassova, J. Smith, C. Pedder, C. Graham, A. Studeny, G. Lysiak-Auvity, A. M. Girard, F. Grave, D. Segal, C. D. Riffkin, G. Pomilio, L. C. Galbraith, B. J. Aubrey, M. S. Brennan, M. J. Herold, C. Chang, G. Guasconi, N. Cauquil, F. Melchiore, N. Guigal-Stephan, B. Lockhart, F. Colland, J. A. Hickman, A. W. Roberts, D. C. Huang, A. H. Wei, A. Strasser, G. Lessene, O. Geneste, The MCL1 inhibitor S63845 is tolerable and effective in diverse cancer models. *Nature*, (2016).
30. A. Letai, S63845, an MCL-1 Selective BH3 Mimetic: Another Arrow in Our Quiver. *Cancer Cell* **30**, 834-835 (2016).
31. N. Cancer Genome Atlas, Comprehensive molecular portraits of human breast tumours. *Nature* **490**, 61-70 (2012).
32. G. Lessene, P. E. Czabotar, B. E. Sleebs, K. Zobel, K. N. Lowes, J. M. Adams, J. B. Baell, P. M. Colman, K. Deshayes, W. J. Fairbrother, J. A. Flygare, P. Gibbons, W. J. Kersten, S.

Kulasegaram, R. M. Moss, J. P. Parisot, B. J. Smith, I. P. Street, H. Yang, D. C. Huang, K. G. Watson, Structure-guided design of a selective BCL-X(L) inhibitor. *Nat Chem Biol* **9**, 390-397 (2013).

33. N. E. Sanjana, O. Shalem, F. Zhang, Improved vectors and genome-wide libraries for CRISPR screening. *Nat Methods* **11**, 783-784 (2014).
34. H. Dai, H. Ding, X. W. Meng, K. L. Peterson, P. A. Schneider, J. E. Karp, S. H. Kaufmann, Constitutive BAK activation as a determinant of drug sensitivity in malignant lymphohematopoietic cells. *Genes Dev* **29**, 2140-2152 (2015).
35. N. Cruickshanks, H. A. Hamed, M. D. Bareford, A. Poklepovic, P. B. Fisher, S. Grant, P. Dent, Lapatinib and obatoclax kill tumor cells through blockade of ERBB1/3/4 and through inhibition of BCL-XL and MCL-1. *Mol Pharmacol* **81**, 748-758 (2012).
36. M. Campone, B. Noel, C. Couriaud, M. Grau, Y. Guillemin, F. Gautier, W. Gouraud, C. Charbonnel, L. Campion, P. Jezequel, F. Braun, B. Barre, O. Coqueret, S. Barille-Nion, P. Juin, c-Myc dependent expression of pro-apoptotic Bim renders HER2-overexpressing breast cancer cells dependent on anti-apoptotic Mcl-1. *Mol Cancer* **10**, 110 (2011).
37. Q. Ding, X. He, J. M. Hsu, W. Xia, C. T. Chen, L. Y. Li, D. F. Lee, J. C. Liu, Q. Zhong, X. Wang, M. C. Hung, Degradation of Mcl-1 by beta-TrCP mediates glycogen synthase kinase 3-induced tumor suppression and chemosensitization. *Mol Cell Biol* **27**, 4006-4017 (2007).
38. R. M. Perciavalle, J. T. Opferman, Delving deeper: MCL-1's contributions to normal and cancer biology. *Trends Cell Biol* **23**, 22-29 (2013).
39. N. Y. Fu, A. C. Rios, B. Pal, R. Soetanto, A. T. Lun, K. Liu, T. Beck, S. A. Best, F. Vaillant, P. Bouillet, A. Strasser, T. Preiss, G. K. Smyth, G. J. Lindeman, J. E. Visvader, EGF-mediated induction of Mcl-1 at the switch to lactation is essential for alveolar cell survival. *Nat Cell Biol* **17**, 365-375 (2015).
40. S. R. Oakes, F. Vaillant, E. Lim, L. Lee, K. Breslin, F. Feleppa, S. Deb, M. E. Ritchie, E. Takano, T. Ward, S. B. Fox, D. Generali, G. K. Smyth, A. Strasser, D. C. Huang, J. E. Visvader, G. J. Lindeman, Sensitization of BCL-2-expressing breast tumors to chemotherapy by the BH3 mimetic ABT-737. *Proc Natl Acad Sci U S A* **109**, 2766-2771 (2012).

AUTHOR MANUSCRIPT

41. K. A. Sarosiek, A. Letai, Directly targeting the mitochondrial pathway of apoptosis for cancer therapy with BH3 mimetics: recent successes, current challenges and future promise. *FEBS J*, (2016).
42. J. Chen, S. Jin, V. Abraham, X. Huang, B. Liu, M. J. Mitten, P. Nimmer, X. Lin, M. Smith, Y. Shen, A. R. Shoemaker, S. K. Tahir, H. Zhang, S. L. Ackler, S. H. Rosenberg, H. Maecker, D. Sampath, J. D. Leverson, C. Tse, S. W. Elmore, The Bcl-2/Bcl-X(L)/Bcl-w inhibitor, navitoclax, enhances the activity of chemotherapeutic agents in vitro and in vivo. *Mol Cancer Ther* **10**, 2340-2349 (2011).
43. J. D. Leverson, D. C. Phillips, M. J. Mitten, E. R. Boghaert, D. Diaz, S. K. Tahir, L. D. Belmont, P. Nimmer, Y. Xiao, X. M. Ma, K. N. Lowes, P. Kovar, J. Chen, S. Jin, M. Smith, J. Xue, H. Zhang, A. Oleksijew, T. J. Magoc, K. S. Vaidya, D. H. Albert, J. M. Tarrant, N. La, L. Wang, Z. F. Tao, M. D. Wendt, D. Sampath, S. H. Rosenberg, C. Tse, D. C. Huang, W. J. Fairbrother, S. W. Elmore, A. J. Souers, Exploiting selective BCL-2 family inhibitors to dissect cell survival dependencies and define improved strategies for cancer therapy. *Sci Transl Med* **7**, 279ra240 (2015).
44. G. R. Anderson, S. E. Wardell, M. Cakir, L. Crawford, J. C. Leeds, D. P. Nussbaum, P. S. Shankar, R. S. Soderquist, E. M. Stein, J. P. Tingley, P. S. Winter, E. K. Zieser-Misenheimer, H. M. Alley, A. Yllanes, V. Haney, K. L. Blackwell, S. J. McCall, D. P. McDonnell, K. C. Wood, PIK3CA mutations enable targeting of a breast tumor dependency through mTOR-mediated MCL-1 translation. *Sci Transl Med* **8**, 369ra175 (2016).
45. J. L. Rinkenberger, S. Horning, B. Klocke, K. Roth, S. J. Korsmeyer, Mcl-1 deficiency results in peri-implantation embryonic lethality. *Genes Dev* **14**, 23-27 (2000).
46. A. R. Delbridge, S. Grabow, A. Strasser, D. L. Vaux, Thirty years of BCL-2: translating cell death discoveries into novel cancer therapies. *Nat Rev Cancer* **16**, 99-109 (2016).
47. X. Wang, M. Bathina, J. Lynch, B. Koss, C. Calabrese, S. Frase, J. D. Schuetz, J. E. Rehg, J. T. Opferman, Deletion of MCL-1 causes lethal cardiac failure and mitochondrial dysfunction. *Genes Dev* **27**, 1351-1364 (2013).
48. R. M. Perciavalle, D. P. Stewart, B. Koss, J. Lynch, S. Milasta, M. Bathina, J. Temirov, M. M. Cleland, S. Pelletier, J. D. Schuetz, R. J. Youle, D. R. Green, J. T. Opferman, Anti-apoptotic MCL-1 localizes to the mitochondrial matrix and couples mitochondrial fusion to respiration. *Nat Cell Biol* **14**, 575-583 (2012).

49. J. Belmar, S. W. Fesik, Small molecule Mcl-1 inhibitors for the treatment of cancer. *Pharmacol Ther* **145**, 76-84 (2015).
50. F. Llambi, T. Moldoveanu, S. W. Tait, L. Bouchier-Hayes, J. Temirov, L. L. McCormick, C. P. Dillon, D. R. Green, A unified model of mammalian BCL-2 protein family interactions at the mitochondria. *Mol Cell* **44**, 517-531 (2011).
51. D. Yecies, N. E. Carlson, J. Deng, A. Letai, Acquired resistance to ABT-737 in lymphoma cells that up-regulate MCL-1 and BFL-1. *Blood* **115**, 3304-3313 (2010).
52. M. F. van Delft, A. H. Wei, K. D. Mason, C. J. Vandenberg, L. Chen, P. E. Czabotar, S. N. Willis, C. L. Scott, C. L. Day, S. Cory, J. M. Adams, A. W. Roberts, D. C. Huang, The BH3 mimetic ABT-737 targets selective Bcl-2 proteins and efficiently induces apoptosis via Bak/Bax if Mcl-1 is neutralized. *Cancer Cell* **10**, 389-399 (2006).

AUTHOR MANUSCRIPT

Acknowledgments: We are grateful to Lorraine O'Reilly and Andreas Strasser for providing antibodies, Leanne Taylor and the Royal Melbourne Hospital Tissue Bank staff for expert technical support, Kim Birchall and Leanne Scott for animal care, Lin Tai and Andrew Kueh for assistance with the CRISPR-Cas9 library screen, and Stefan Glaser who provided the MCL-1 retrovirus construct. Coded primary breast tumor samples were provided by the Victorian Cancer Biobank (supported by the Victorian Government), which provided coded breast tissue and data. **Funding:** This work was supported by the National Health and Medical Research Council, Australia (NHMRC, 1016701, 1040978, 1086727 and 1101378); NHMRC IRIISS; the Victorian State Government through Victorian Cancer Agency funding (TRP13041) and Operational Infrastructure Support; the Australian Cancer Research Foundation; The National Breast Cancer Foundation (NT-13-06); Servier; The Qualtrough Cancer Research Fund and The Joan Marshall Breast Cancer Research Fund. D.M. was supported by a NBCF Early Career Fellowship and NHMRC Project Grant (1101378); J.R.W. by an NHMRC/NBCF Research Fellowship and the RACP; B.P. by a Victorian Cancer Agency Early Career Seed Grant (13-035) and NHMRC Project Grant (1100807); N.L. by a Worldwide Cancer Research grant (15-0042); J.E.V. by an NHMRC Australia Fellowship (1037230) and Research Fellowship (1102742); D.C.S.H. and G.J.L by NHMRC Research Fellowships (1043149 and 1078730, respectively). **Author contributions:** All the authors were involved in the data analysis and interpretation. D.M., J.R.W., F.V., J.E.V. and G.J.L. planned the project; D.M., J.R.W., F.V. designed and performed

the experiments and analysed the data; J.G. provided and analyzed the CRISPR clones, A.L.M., M.C., E.S., and O.G. provided S63845 compound and expert advice on its application in the PDX models; B.P., G.G. and G.S. performed the RNAseq analysis; X.L. and G.D. analyzed BAK activation in PDXs, A.S., J.G. and N.L. performed some western blots and toxicity assays; D.S., M.H., D.C.S.H., and G.L. contributed expertise and experimental reagents; K.L. performed immunostaining; D.M., J.R.W., J.E.V. and G.J.L. wrote the paper. **Competing interests:** A.L.M., M.C., E.S., O.G. are employees of Servier. Servier has filed patents on S63845 in relation to cancer therapy (Kotschy et al, Nature 2016) and holds the IP on S63845 *(29)*. D.M., J.R.W., F.V., A.S., J.N.G., G.G., X.L., G.D., K.L., N.L., D.S., M.H., D.C.S.H., G.S., G.L., J.E.V., and G.J.L. are employees of The Walter and Eliza Hall Institute, which has received research funding from Servier and receives milestone payments from Abbvie and Genentech in relation to venetoclax (ABT-199).

FIGURE LEGENDS

Fig. 1. MCL-1 and BCL-2 expression in PDX tumors and in vitro sensitivity to S63845 in cell lines and PDX models. (**A**) Box-plots showing the relative expression (log2-RPKM) of BCL-2, MCL-1, BCL-XL, and BCL-W across breast tumor subtypes. *BRCA1*-mutant TNBC, n = 6; ER, n = 6; HER2, n = 8; TNBC (*BRCA1* wt), n = 10. (**B**) Western blot analysis of estrogen receptor (ER) and BH3 family member (MCL-1, BCL-2, BCL-XL, BAX, BAK, BIM, and BID) protein expression in PDX models (2 independent tumors per PDX). Tubulin was used as a loading control. Arrowhead indicates MCL-1 band. B1, *BRCA1*-mutated; (**C**) Cell lines were treated at increasing concentrations of S63845 for 24 hours before assessment of viability using CellTiter-Glo. Shown are mean ± s.e.m. for n≥3 independent experiments. (**D**) Western blot showing the expression of BCL-2 family members in breast cancer cell lines. HSP70 was used as loading control. (**E**) HER2-amplified and TNBC PDX tumor cells were cultured for 24 hours in mammosphere medium in the presence of ABT-737 (1 μM), ABT-199 (1 μM), WEHI-539 (1 μM), or S63845 (1 μM), and viability was determined compared to DMSO vehicle control. Shown are mean ± s.e.m. The number of independent experiments is indicated. B1, *BRCA1*-mutated; ND, Not determined.

Fig. 2. Resistance to S63845-induced apoptosis through loss of BAK or elevated BCL-XL. (**A**) SK-BR-3 cells were infected with a genome-wide lentiviral sg RNA library, treated with S63845 (1 μM) or DMSO control, and then gDNA of surviving cells was isolated to identify the sgRNAs by NGS. Shown is the pooled analysis from six independent infections, displaying normalized values for S63845 or DMSO control. Solid red bar represents the regression line. The sgBAK1 hits are shown as blue dots. See table S5 for top upregulated sgRNAs in the S63845 treated pools. (**B**) SK-BR-3 cells infected with CRISPR-Cas9 guides targeting pro-apoptotic proteins were treated with increasing concentrations of S63845 for 24 hours before assessment of viability using CellTiter-Glo. Ev, Empty vector. (**C**) SK-BR-3 cells infected with CRISPR-Cas9 guides targeting BIM, BID, and PUMA as shown were treated with increasing concentrations of S63845, as described above. (**D**) The MDA-MB-468 cell line was treated with increasing concentrations of S63845 in the presence of ABT-199, WEHI-539, or ABT-737 (500 nM) for 24 hours before assessment of viability using CellTiter-Glo. For B-D, shown are mean ± s.e.m. for 3

AUTHOR MANUSCRIPT

independent experiments. (**E**) PDX tumor cells were cultured for 24 hours in mammosphere medium with S63845, ABT-199, ABT-737, WEHI-539, and S63845 (500 nM and 1 μM) or combination treatment with S63845 and other BH3 mimetics (both at 500 nM) before assessment of viability using CellTiter-Glo. Results are presented as percentages of untreated cells. Bars represent mean ± s.e.m. for at least 5 independent experiments per PDX. The tumor subtype for each PDX is shown in parentheses. B1, *BRCA1*-mutated.

Fig. 3. Synergistic effect of S63845 with lapatinib, trastuzumab, or docetaxel. (**A**) SK-BR-3 cells were treated with lapatinib (500 nM), trastuzumab (100 μg/mL), docetaxel (2 nM), or left untreated in the presence of S63845 (30 nM), with or without Q-VD-OPh (QVD, 10 μM) for 72 hours before viability analysis with propidium iodide (PI) staining. Results are presented as a percentage of untreated cells and represent 3-5 independent experiments. Shown are mean ± s.e.m. for 3-5 independent experiments. (**B** and **C**) SK-BR-3 cells were treated with increasing concentrations of S63845 and docetaxel (**B**), or HER2-targeted therapies lapatinib (left panel) for 72 hours or trastuzumab (right panel) for 96 hours (**C**), then subjected to viability assays using CellTiter-Glo followed by BLISS score analysis. BLISS synergy values are > 0.0 on vertical axis. * $p < 0.05$; ** $p < 0.005$; *** $p < 0.001$. (**D**) Western blot analysis of lysates from (A) showing expression of MCL-1, BCL-XL, BAK, BAX, BIM, BID, AKT, P-AKT, ERK, P-ERK, and cleaved caspase 3 (CC3). Tubulin was used as a loading control.

Fig. 4. Improved tumor response to docetaxel in TNBC and trastuzumab in HER2-amplified PDX models with the addition of S63845. Kaplan-Meier survival curves (left panels) and tumor volume curves (right panels) for PDX models. (**A**) TNBC PDX 110, from a *BRCA1* mutation carrier (n = 10-12 mice per arm) and (**B**) TNBC PDX 838 (n = 10-11 mice per arm). Mice were treated with vehicle alone (black line), docetaxel (10 mg/kg i.p. on day 1 and 22) plus vehicle for S63845 (blue line), S63845 (25 mg/kg i.v. once weekly for 6 weeks, on days 2, 9, 16, 23, 30, and 37) plus vehicle for docetaxel (green line), or combined docetaxel and S63845 (red line). (**C**) HER2-amplified PDX 231 (n = 6-8 per arm). Mice were treated with vehicle (black line), trastuzumab (30 mg/kg loading dose on day 1, then 15 mg/kg twice weekly for 6 weeks starting on day 4) plus vehicle for S63845 (blue line), S63845 (25 mg/kg once weekly for 6 weeks on days 2, 9, 16, 23, 30, and 37) plus vehicle for trastuzumab (green line), or

combined trastuzumab and S63845 (red line). For tumor volume curves, black bars indicate the total duration of the treatment. Mice, which remained otherwise healthy, were sacrificed when tumor size reached the experimental ethical endpoint (>600 mm^3). Shown are mean ± s.e.m. Log rank (Mantel-Cox) p value is shown for combination therapy versus docetaxel or trastuzumab alone. Tumor growth curves for individual mice from PDX models 110, 838, and 231 are shown in fig. S10.

AUTHOR MANUSCRIPT

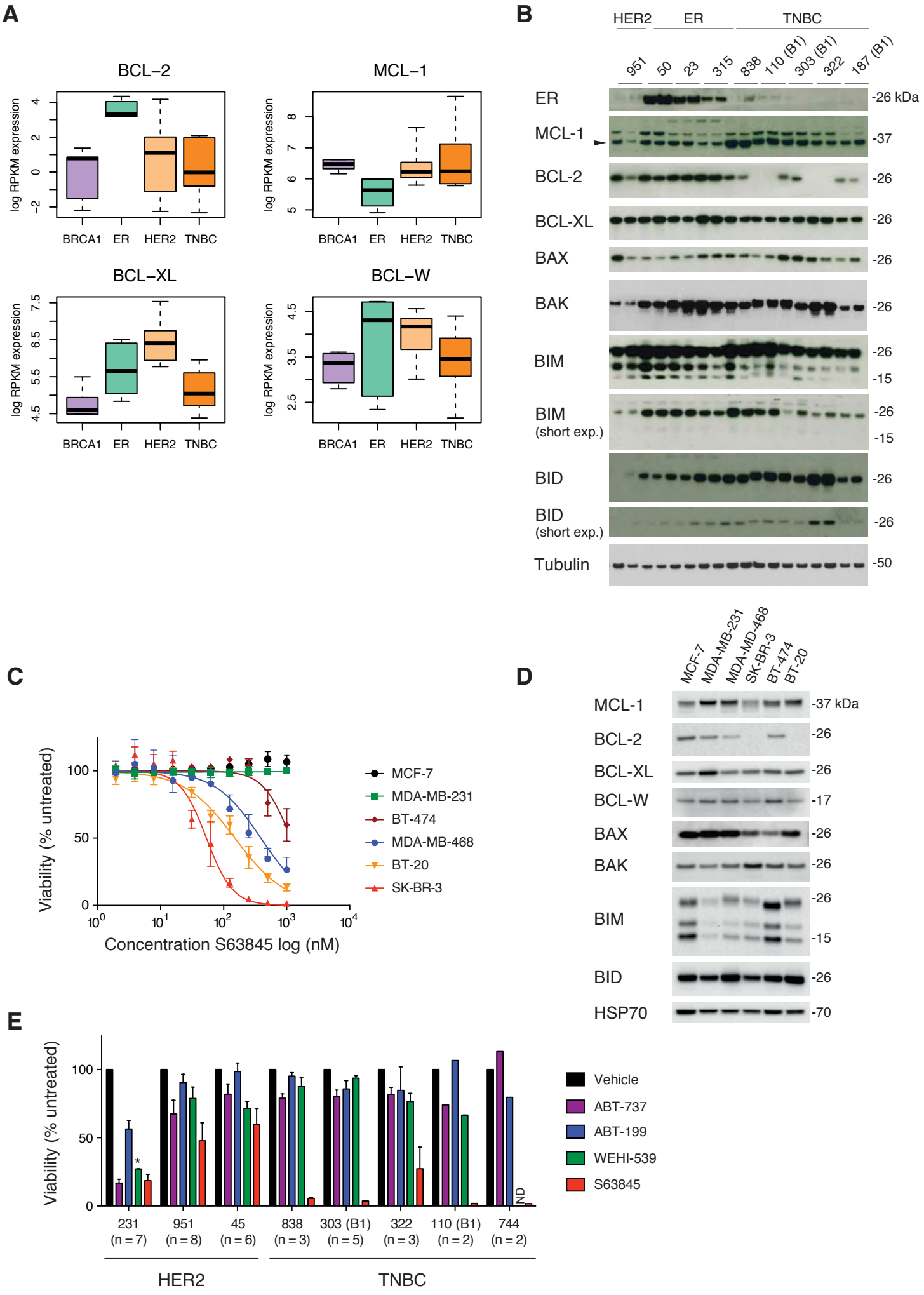
A
BCL−2
MCL−1
BCL−XL
BCL−W
log RPKM expression
BRCA1
ER
HER2
TNBC
B
HER2
ER
TNBC
951
50
23
315
838
110 (B1)
303 (B1)
322
187 (B1)
ER
MCL-1
BCL-2
BCL-XL
BAX
BAK
BIM
BIM (short exp.)
BID
BID (short exp.)
Tubulin
-26 kDa
-37
-26
-15
-50
C
Viability (% untreated)
Concentration S63845 log (nM)
MCF-7
MDA-MB-231
BT-474
MDA-MB-468
BT-20
SK-BR-3
D
MCF-7
MDA-MB-231
MDA-MD-468
SK-BR-3
BT-474
BT-20
MCL-1
BCL-2
BCL-XL
BCL-W
BAX
BAK
BIM
BID
HSP70
-37 kDa
-26
-17
-15
-70
E
Viability (% untreated)
231 (n = 7)
951 (n = 8)
45 (n = 6)
838 (n = 3)
303 (B1) (n = 5)
322 (n = 3)
110 (B1) (n = 2)
744 (n = 2)
ND
HER2
TNBC
Vehicle
ABT-737
ABT-199
WEHI-539
S63845

Figure 1

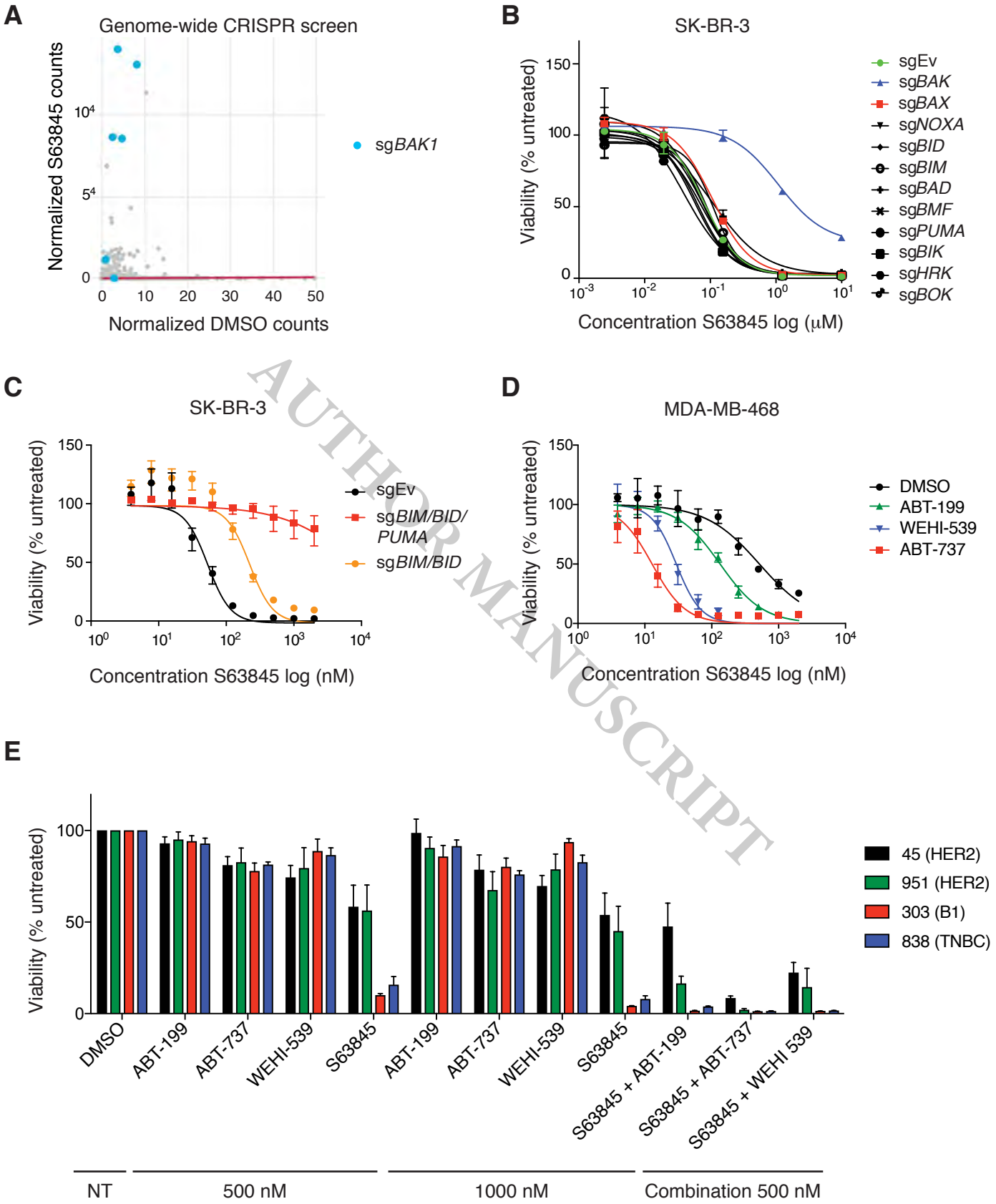

AUTHOR MANUSCRIPT

Figure 2

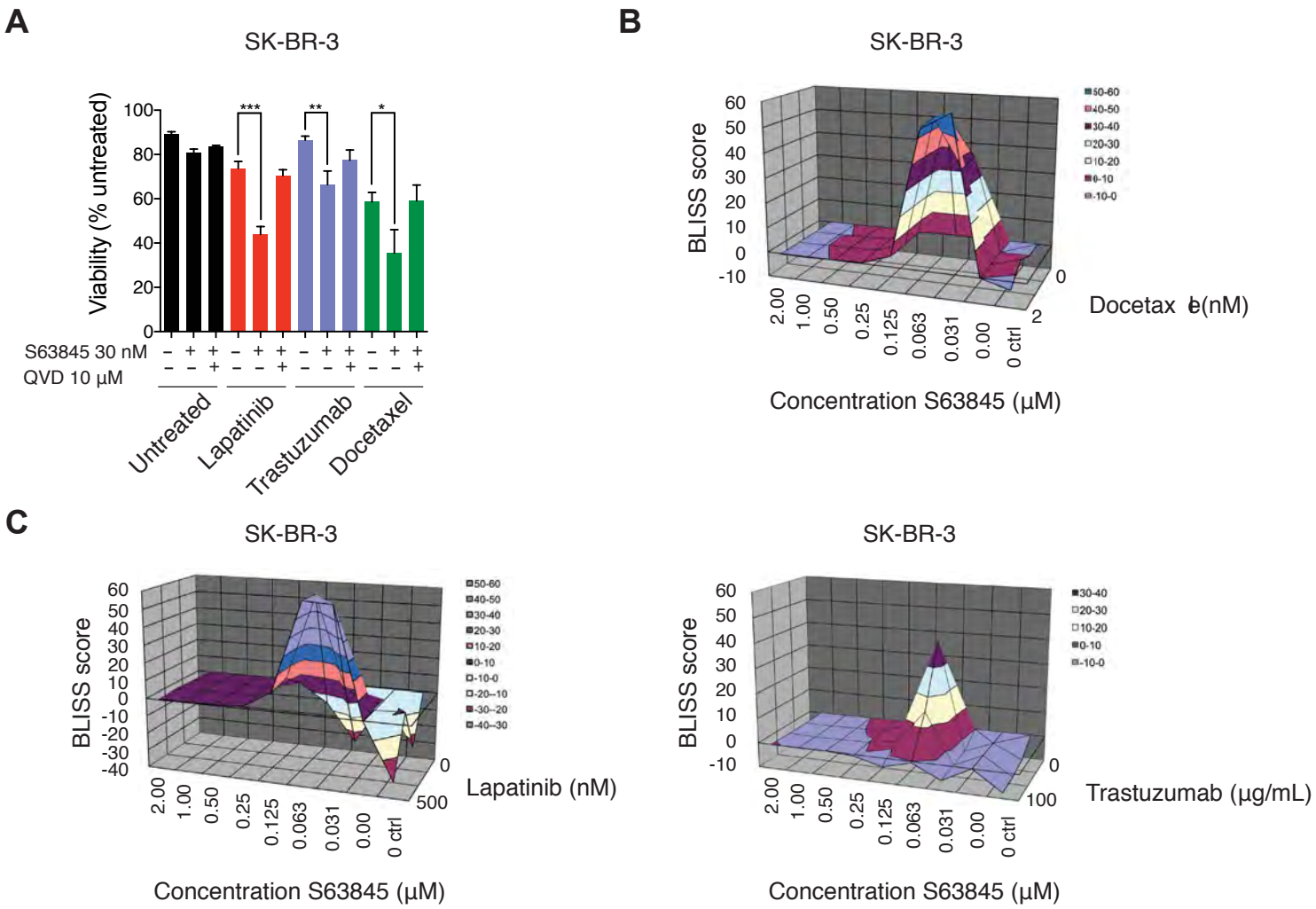
A
SK-BR-3
Viability (% untreated)
100
80
60
40
20
0
***
**
*
S63845 30 nM
QVD 10 µM
Untreated
Lapatinib
Trastuzumab
Docetaxel
B
SK-BR-3
BLISS score
60
50
40
30
20
10
0
-10
50-60
40-50
30-40
20-30
10-20
0-10
-10-0
2.00
1.00
0.50
0.25
0.125
0.063
0.031
0.00
0 ctrl
Concentration S63845 (µM)
Docetaxel (nM)
C
SK-BR-3
BLISS score
60
50
40
30
20
10
0
-10
-20
-30
-40
50-60
40-50
30-40
20-30
10-20
0-10
-10-0
-20--10
-30--20
-40--30
Lapatinib (nM)
500
Concentration S63845 (µM)
SK-BR-3
BLISS score
30-40
20-30
10-20
0-10
-10-0
Trastuzumab (µg/mL)
100
Concentration S63845 (µM)
D
Untreated
Lapatinib
Trastuzumab
Docetaxel
S63845 30 nM
QVD 10 µM
MCL-1
BCL-XL
BAK
BAX
BIM
BID
AKT
P-AKT
ERK
P-ERK
CC3
Tubulin
37 kDa
26
26
26
26
15
26
60
60
42
42
30
20
48

Figure 3

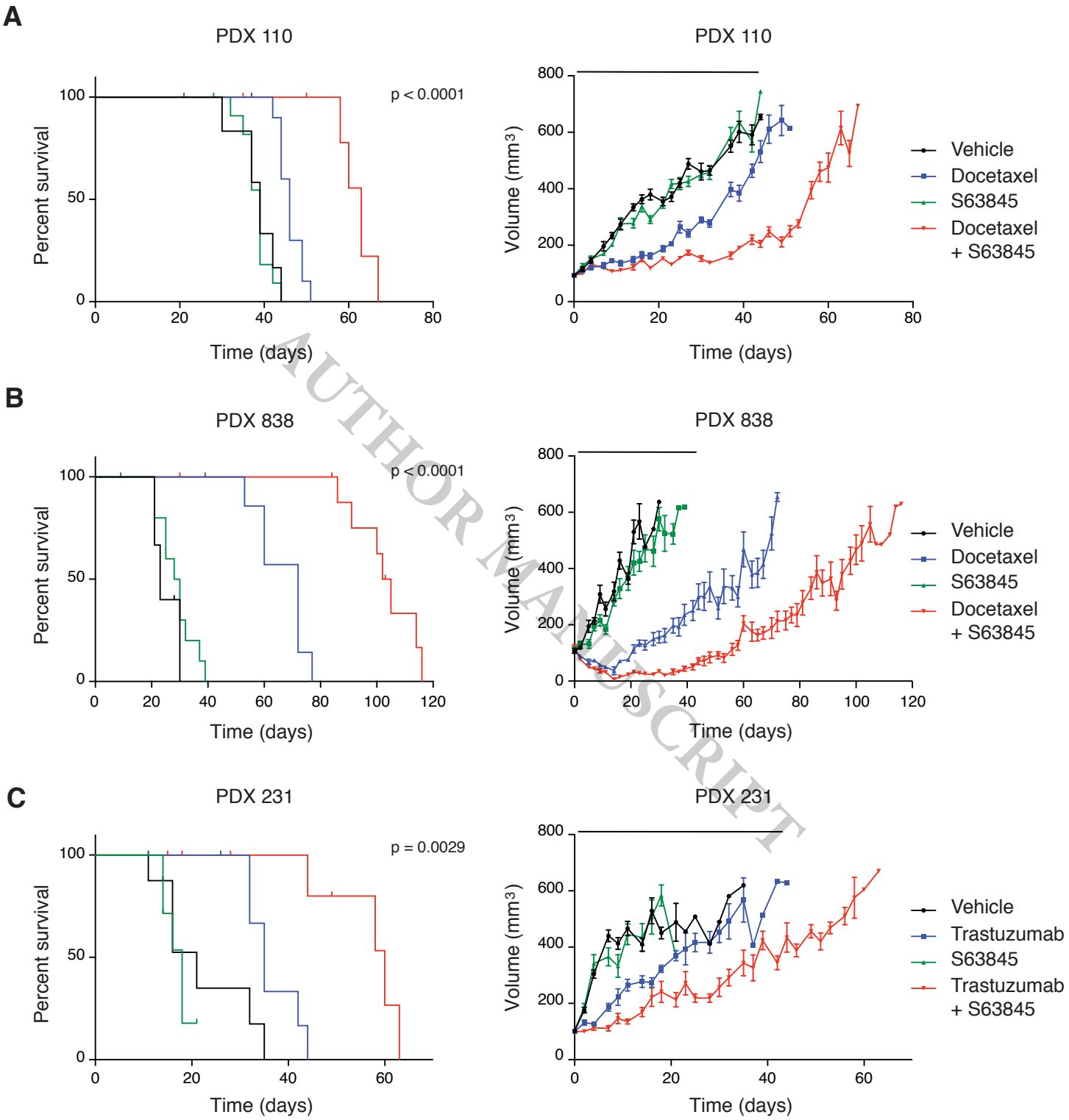

AUTHOR MANUSCRIPT

Figure 4

Supplementary Materials for

Synergistic action of the MCL-1 inhibitor S63845 with current therapies in preclinical models of triple negative and HER2-amplified breast cancer

Delphine Merino, James R. Whittle, François Vaillant, Antonin Serrano, Jia-Nan Gong, Goknur Giner, Ana Leticia Maragno, Maïa Chanrion, Emilie Schneider, Bhupinder Pal, Xiang Li, Grant Dewson, Julius Gräsel, Kevin Liu, Najoua Lalaoui, David Segal, Marco J. Herold, David C.S. Huang, Gordon K. Smyth, Olivier Geneste, Guillaume Lessene, Jane E. Visvader*, Geoffrey J. Lindeman*

*Corresponding authors. Email: visvader@wehi.edu.au (J.E.V.), lindeman@wehi.edu.au (G.J.L.)

The PDF file includes:

Materials and Methods

References (10, 33, 40, 53-66)

Fig. S1. Expression of BCL-2 family members and sensitivity to S63845 or A-1210477.

Fig. S2. RNAseq analysis of BCL-2 family members in PDX models.

Fig. S3. Expression of *BCL-XL*, *BCL-2*, *BCL-W* and *MCL-1* in METABRIC and TCGA databases.

Fig. S4. Characterization of ER, PR, HER2, and BCL-2 family member protein expression in PDX models by immunohistochemistry.

Fig. S5. Deep sequencing of genome-wide lentiviral sgRNA libraries, knockdown of BH3 proteins and S63845 mediated disruption of MCL-1 complexes containing BH3-only proteins.

Fig. S6 Generation and analysis of S63845 resistant cell lines.

Fig. S7. Exploring molecular mechanisms of resistance to S63845.

Fig. S8. Effect of concomitant treatment of SK-BR-3 cells with a BH3 mimetic and trastuzumab, lapatinib or docetaxel.

Fig. S9. Role of BIM in the synergistic effect of S63845.

Fig. S10. Individual tumor growth curves in TNBC and HER2-amplified PDXs after treatment with S63845 and docetaxel or trastuzumab.

Fig. S11. Effect of combination therapy on tumor cell death.

Fig. S12 Effect of combination therapy on mouse weight, biochemistry and blood counts.

Table S1. Clinical, histopathological and molecular features of primary breast tumors.

Other Supplementary Material for this manuscript includes the following (Microsoft Excel format):

Table S2. BCL-2 family mRNA expression in PDX models.

Table S3. Statistical analysis of gene expression between different molecular subtypes of breast cancer in PDX models.

Table S4. Statistical analysis of *MCL-1*, *BCL-2*, *BCL-XL* and *BCL-W* gene expression between different molecular subtypes of breast cancer in METABRIC and TCGA datasets.

Table S5. Normalized sgRNA counts upregulated in S63845 treated cells compared to DMSO control.

Table S6. Primers used for sequencing CRISPR clones.

Table S7. Sequencing analysis of CRISPR clones for *BAK*, *BAX, BMF,* and *NOXA*.

AUTHOR MANUSCRIPT

Materials and Methods

Cell-lines and viability assays

The breast cancer cell lines MCF-7, BT-20, MDA-MB-231, MDA-MB-468, SK-BR-3, and BT-474 were maintained in RPMI-1640 plus GlutaMAX-1 (Gibco) supplemented with 10% fetal calf serum (FCS) and 10 µg/ml insulin. HEK293T cells were maintained in DMEM plus GlutaMAX-1 (Gibco) supplemented with 10% fetal calf serum. For viability assays, cells were plated at 2 x 10^5 cells/ml in 96 well plates, in RPMI-1640 medium (Gibco) supplemented with 10% FCS and 10 µg/ml insulin, and treated with increasing concentrations of S63845 (Servier), ABT-737 (Selleckchem), ABT-199 (Active Biochemku), and WEHI-539 (WEHI). For tumor sphere assays, single cell suspensions were obtained by digestion of primary tumors and sorted as previously described (*10, 40*). Sorted cells were cultured in mammosphere medium (*53*).

Cell viability was assessed using the CellTiter-Glo Luminescent Assay (Promega) as per the manufacturer's instructions. The broad-spectrum caspase inhibitor Q-VD-OPh hydrate (Sigma-Aldrich) was used at 10 µM. Propidium iodide exclusion (5 µg/ml) was analyzed by flow cytometry. For in vitro cell assays to address synergy between different drugs, combination effects were determined using the Bliss independence method (*54*).

In vivo experiments

Human breast cancer tissues were obtained from consenting patients through the Royal Melbourne Hospital Tissue Bank and the Victorian Cancer Biobank with relevant institutional review board approval. Human ethics approval was obtained from the Walter and Eliza Hall Institute (WEHI) Human Research Ethics Committee. NOD-SCID-IL2R$\gamma^{-/-}$ mice were bred and maintained according to institutional guidelines. Animal experiments were approved by the WEHI Animal Ethics Committee.

Human PDXs and Tumor Monitoring

Cohorts of 36–42 female mice were seeded with thawed single cell suspensions of early passage human breast tumors (passage 2 or 3). Briefly, 150,000–250,000 cells were resuspended in 10 µl of transplantation buffer (50% fetal calf serum, 10% of a 0.04% trypan blue solution, and 40% PBS) and growth-factor-reduced Matrigel [BD] at a ratio of 3:1, and injected into the cleared mammary fat pads of 3- or 4-week-old NOD-SCID-IL2R $\gamma_c^{-/-}$ female mice. Mice were monitored for tumor development three times weekly and tumor size measured using electronic vernier calipers. Tumor volume was

estimated by measuring the minimum and maximum tumor diameters using the formula: (minimum diameter)^2(maximum diameter)/2. Once tumors reached a volume of 80-120 mm^3, mice were randomized into treatment arms and treatment commenced. Randomization and tumor measurements were managed using the Study Director software (v 3.0, studylog). Mice were sacrificed at the first measurement where tumor volume exceeded 600 mm^3, or if their health deteriorated for reasons other than disease progression or drug toxicity (censored event). Although >10% weight loss was a pre-defined censoring event, no mice in the treatment cohorts lost weight.

S63845 (25 mg/kg) or vehicle were injected i.v. weekly for six weeks. Vehicle for S63845 was 20% (*2*-Hydroxypropyl)-β-cyclodextrin and 25 mM hydrochloric acid. Docetaxel or vehicle (PBS) were prepared as previously described (*40*) and injected i.p. every 21 days for two treatment cycles. Trastuzumab or vehicle (PBS) were injected i.p. twice weekly. Mice received a loading dose (30 mg/kg) on day 1, followed by twice weekly maintenance dose (15 mg/kg) starting on day 4. Mice were monitored as per institutional guidelines.

AUTHOR MANUSCRIPT

Toxicity data

Blood was collected by cardiac puncture 21 days after start of treatment in microcuvette (Sarstedt) and microtainer tubes (BD Pharmingen). Full blood examination was carried out on an Advia 2120 blood analysis machine (Siemens) and serum analysis on an Architect auto-analyser (Abbott) after serum separation according to the manufacturer's instructions.

Immunohistochemistry

PDX tumors were collected and fixed in 4% paraformaldehyde before embedding in paraffin. Sections were subjected to antigen retrieval using pH9 antigen retrieval buffer (DAKO S2375) at 95°C for 20 min (or citrate buffer pH6 at 95°C for 20 min for CC3) and then incubated with antibodies against ER (NCL-L-ER-6F11, Novocastra), PR (NCL-L-PGR-312, Novocastra), HER2 (SP3, Spring Bioscience), cytokeratin 5 (NCL-L-CK5, Novocastra), BCL-2 (BCL-2–100, WEHI antibody facility), MCL-1 (D35A5, Cell Signaling), BIM (C34C5, Cell Signaling), BCL-XL (54H6, Cell Signaling), or BAK (polyclonal, Sigma), or anti-cleaved caspase 3 (CS-9664, Cell Signaling) at 4ºC overnight, followed by biotinylated anti-IgG secondary antibodies (Vector Labs). Signal detection was performed using ABC Elite (Vector Labs) for 30 min and 3,3′-diaminobenzidine (Dako) for 5 min at room temperature.

Immunoblot analysis

Tumors were homogenized in lysis buffer (20 mM Tris.HCL, 135 mM NaCl, 1.5 mM $MgCl_2$, 1 mM EGTA, 1% Triton X-100, and 10% glycerol). Protein lysates were analyzed by Western blot on 12% SDS-polyacrylamide gels (Invitrogen) and transferred onto PVDF membranes (Millipore). Membranes were probed with primary antibodies: anti-ER (c-542, Santa Cruz), anti-BCL-2 (Bcl-2-100, WEHI Monoclonal Antibody Facility), anti-BCL-XL (54H6, Cell Signaling Technologies), anti-MCL-1 (14C11-20, WEHI Monoclonal Antibody Facility), anti-BIM (C34C5, Cell Signaling Technologies; 10B12, ENZO), anti-BAX (A7, WEHI Monoclonal Antibody Facility), anti-BAK (A4, WEHI Monoclonal Antibody Facility), anti-cleaved caspase 3 (CS-9661, Cell Signaling), anti-BID (WEHI Monoclonal Antibody Facility), anti-PUMA (ProSci), anti-BCL-W (16H12, WEHI Monoclonal Antibody Facility) (*55*), anti-ERK, anti-P-ERK, anti-AKT, anti-P-AKT (Ser473) (all from Cell Signaling Technologies), anti-EE (BabCO), anti-HA (3F10, Roche), anti–FLAG (9H1, WEHI), anti-HSP70 (N6, WEHI monoclonal antibody laboratory), and anti-tubulin (DM1A, Sigma-Aldrich). After primary antibody, membranes were probed using HRP-conjugated anti-IgG secondary antibodies and ECL (GE Healthcare Life Sciences).

Immunoprecipitation studies

Cell suspensions from PDX 838 were obtained by digestion of primary tumors, sorted, and cultured for 5 hours in mammosphere medium (as described above) in the absence or presence of 4 μM of S63845. Cells were then lysed in lysis buffer (20 mM Tris.HCL, 135 mM NaCl, 1.5 mM $MgCl_2$, 1 mM EGTA, 1% Triton X-100, and 10% glycerol), and 500 μg of lysates were precleared by incubation with protein G sepharose for 1 hour at 4°C and then immunoprecipitated with 5 μg of anti-MCL-1 (SC819, Santa-Cruz Biotechnology) antibody and protein G-sepharose. Beads were washed, and immunoprecipitate was eluted in SDS-sample buffer before western blot analysis.

For co-expression and co-immunoprecipitation experiments, HEK293T cells were transfected with a FLAG-tagged MCL-1 and HA-tagged (BID, BIM, BAK, PUMA, BAX, BAD) or EE-tagged (BMF, NOXA) constructs. Cells were treated with S63845 (5 μM) or DMSO for 5 hours before lysis and preclearing using sepharose beads. Co-immunoprecipitation of FLAG tagged proteins was performed overnight using anti-FLAG mAb-coupled agarose beads before washes, elution, and western blot analysis.

Mitochondrial isolation and cytochrome *c* release

To assess the subcellular localization of BAK, cells from PDX45 and 744 were washed with 1 ml PBS at 1,500 rpm for 5 min at room temperature after cell counting. Cell pellet was then permeabilized in permeabilization buffer (20 mM Hepes KOH pH 7.5, 93 mM sucrose, 100 mM KCl, 2.5 mM $MgCl_2$) with 0.025% digitonin (w/v) in the presence of complete protease inhibitor for 10 min on ice at a concentration of 10 million cells per ml. Heavy membrane fraction was then separated from cytosolic fraction by centrifugation of permeabilized sample at 13,000 rpm for 5 min at 4°C.

The mitochondrial fraction obtained as described above was used to study BAK activation on the mitochondrial outer membrane (sub-cellular localization test). The mitochondria-containing heavy membrane fraction was resuspended in permeabilization buffer with complete protease inhibitor at a concentration of 10 million cells per ml. Recombinant full length caspase-8 cleaved tBid or MCL-1 inhibitor was added to the membrane fraction at the indicated dose to incubate for 30 min at 30°C to activate BAK on the mitochondrial outer membrane. After activation, samples were centrifuged at 13,000 rpm for 5 min at RT to separate the supernatant (containing released cytochrome *c*) and the membrane fraction. Both fractions were then treated with SDS sample buffer with 5% 2-mercaptoethanol and heated at 100°C for 5 min to prepare for SDS-PAGE.

AUTHOR MANUSCRIPT

Illumina MiSeq sequencing

PDX tissues were homogenized and total RNA extracted using RNAeasy mini kit (Qiagen). The RNA (50 ng) samples were prepared and indexed for Illumina sequencing using the TruSeq RNA V2 sample Prep Kit (Illumina) as per manufacturer's instruction. The library was quantified using the Agilent Tapestation and the Qubit RNA assay kit for Qubit 2.0 Fluorometer (Life Technologies). The indexed libraries were then prepared for paired end 75 bp sequencing on a NextSeq500 instrument using the 150 cycle kit v2 chemistry (Illumina) as per manufacturer's instructions.

Lentiviral retroviral constructs and sgRNA design

SK-BR-3 cells were serially infected with lentiviruses expressing Cas9 mCherry and sgRNA GFP. Constitutive Cas9 and inducible guide RNA vectors have been described (*56*). $mCherry^+$ GFP^+ cells were sorted by flow cytometry (BD Biosciences). To induce expression of the sgRNA, doxycycline was added to the tissue culture medium at a final concentration of 1 μg/ml. After 72 hours, cell lysates were prepared for Western blot analysis. In addition, genomic DNA was sequenced to confirm the

mutation of targeted DNA by using the Illumina MiSeq platform. For sequencing, we used PCR primers with overhang sequences for each sgRNA (table S6), as previously described (*56*). Results obtained for BAK, BAX, BMF, and NOXA are detailed in table S7.

BIM KO clones and BID KO clones were generated after sg*BIM* or sg*BID* infection in Cas9 SK-BR-3, treatment with doxycycline, and sorting of single cells in 96 well plates. The expression of proteins was assessed by western blot analysis, and mutations were confirmed by sequencing. For the Cas9 sg*BIM/BID/PUMA* deficient SK-BR-3 cells, BIM, BID, PUMA CRISPR guides were transfected into Cas9 SK-BR-3. In addition, BIM/BID/PUMA deficient cells were also generated by the infection of BIM KO cells with BID and PUMA CRISPR guides. BIM/BID double KO clones were generated by infection of BIM KO clones with two different sg*BID* guides, single cell sorting, and selection of double KO clones by western blot analysis. Cells were treated with doxycycline and selected for 72 hours with 1 μM of S63845. All the BIM KO and Cas9 SK-BR-3 cells died during this process, whereas many BIM/BID/BIM SK-BR-3 clones survived. Western blot confirmed BIM, BID, and PUMA down-regulation, and the clones were resistant to S63845.

For MCL-1 overexpression studies, the MSCV-MCL1-IRES-GFP was used as previously described (*57*). SK-BR-3 cells were infected and GFP infected cells were sorted before western blot analysis and toxicity assays.

CRISPR-Cas9 genome-wide screen

SK-BR-3 Cas9 expressing cells were maintained as described above. 1.5 x 10^6 cells were plated in T75 flasks, and three days later they were infected at low MOI with the human genome-wide gRNA lentiviral library (Addgene #1000000048) (*33*) in six independent infections. Three days after infection, each of the SK-BR-3 Cas9 expressing sgRNA library transduced cells were treated with 1 μM S63845, DMSO control, or medium alone. S63845 or DMSO control was added every 72 hours. Surviving cells from each treated sample were pooled, and genomic DNA was extracted and used for NGS. We constructed a matrix of counts for sgRNAs and kept the matrix unfiltered. The counts were normalized using TMM normalization with an offset of 0.2 (*58*). Gene-wise Negative Binomial Generalized Linear Models were fitted to obtain average expression values for each sgRNA in Reference and MCL-1 inhibited replicates using edgeR package (version 3.14.0) (*59*). False discovery rates were used together with log2-fold changes to rank genes (*60*).

RNA-seq analysis

RNA from PDX tumors was sequenced on a HiSeq 2000 at the Australian Genome Research Facility, Melbourne. Xenografts were derived from 3-4 patients for each tumor subtype, and each tumor was passaged in 2-4 mice. This produced a total of 30 PDX samples from 13 patients. An average of 20 million 100 bp paired-end reads were obtained per sample. Reads were aligned to the human genome hg19 using Rsubread package 1.16.1 (*61*) and were assigned to Entrez genes using featureCounts (*62*). Library sizes were normalized by Trimmed Median of M-values (*58*). RSEM counts for the TCGA breast cancer tumors were downloaded from https://tcga-data.nci.nih.gov. Expression data from the METABRIC project were downloaded from http://www.compbio.group.cam.ac.uk/publications/supplementary-material. Differential expression analyses used the limma software package (*63*) robust empirical Bayes moderated t-tests (*64*). The PDX and TCGA RNA-seq counts were transformed using the voom method (*65*). The correlation between multiple PDX samples from the same human patient was estimated using the duplicateCorrelation method (*66*).

AUTHOR MANUSCRIPT

REFERENCES

10. F. Vaillant, D. Merino, L. Lee, K. Breslin, B. Pal, M. E. Ritchie, G. K. Smyth, M. Christie, L. J. Phillipson, C. J. Burns, G. B. Mann, J. E. Visvader, G. J. Lindeman, Targeting BCL-2 with the BH3 mimetic ABT-199 in estrogen receptor-positive breast cancer. *Cancer Cell* **24**, 120-129 (2013).
33. N. E. Sanjana, O. Shalem, F. Zhang, Improved vectors and genome-wide libraries for CRISPR screening. *Nat Methods* **11**, 783-784 (2014).
40. S. R. Oakes, F. Vaillant, E. Lim, L. Lee, K. Breslin, F. Feleppa, S. Deb, M. E. Ritchie, E. Takano, T. Ward, S. B. Fox, D. Generali, G. K. Smyth, A. Strasser, D. C. Huang, J. E. Visvader, G. J. Lindeman, Sensitization of BCL-2-expressing breast tumors to chemotherapy by the BH3 mimetic ABT-737. *Proc Natl Acad Sci U S A* **109**, 2766-2771 (2012).
53. G. Dontu, W. M. Abdallah, J. M. Foley, K. W. Jackson, M. F. Clarke, M. J. Kawamura, M. S. Wicha, In vitro propagation and transcriptional profiling of human mammary stem/progenitor cells. *Genes Dev* **17**, 1253-1270 (2003).

54. M. N. Prichard, L. E. Prichard, W. A. Baguley, M. R. Nassiri, C. Shipman, Jr., Three-dimensional analysis of the synergistic cytotoxicity of ganciclovir and zidovudine. *Antimicrob Agents Chemother* **35**, 1060-1065 (1991).
55. L. A. O'Reilly, C. Print, G. Hausmann, K. Moriishi, S. Cory, D. C. Huang, A. Strasser, Tissue expression and subcellular localization of the pro-survival molecule Bcl-w. *Cell Death Differ* **8**, 486-494 (2001).
56. B. J. Aubrey, G. L. Kelly, A. J. Kueh, M. S. Brennan, L. O'Connor, L. Milla, S. Wilcox, L. Tai, A. Strasser, M. J. Herold, An inducible lentiviral guide RNA platform enables the identification of tumor-essential genes and tumor-promoting mutations in vivo. *Cell Rep* **10**, 1422-1432 (2015).
57. Z. Xu, P. P. Sharp, Y. Yao, D. Segal, C. H. Ang, S. L. Khaw, B. J. Aubrey, J. Gong, G. L. Kelly, M. J. Herold, A. Strasser, A. W. Roberts, W. S. Alexander, C. J. Burns, D. C. Huang, S. P. Glaser, BET inhibition represses miR17-92 to drive BIM-initiated apoptosis of normal and transformed hematopoietic cells. *Leukemia* **30**, 1531-1541 (2016).
58. M. D. Robinson, A. Oshlack, A scaling normalization method for differential expression analysis of RNA-seq data. *Genome Biol* **11**, R25 (2010).
59. M. D. Robinson, D. J. McCarthy, G. K. Smyth, edgeR: a Bioconductor package for differential expression analysis of digital gene expression data. *Bioinformatics* **26**, 139-140 (2010).
60. Y. Benjamini, Y. Hochberg, Conrolling the false discovery rate: a practical and powerful approach to mulitple testing. *J Royal Staistical Society Series B* **57**, 289-300 (1995).
61. Y. Liao, G. K. Smyth, W. Shi, The Subread aligner: fast, accurate and scalable read mapping by seed-and-vote. *Nucleic Acids Res* **41**, e108 (2013).
62. Y. Liao, G. K. Smyth, W. Shi, featureCounts: an efficient general purpose program for assigning sequence reads to genomic features. *Bioinformatics* **30**, 923-930 (2014).
63. M. E. Ritchie, B. Phipson, D. Wu, Y. Hu, C. W. Law, W. Shi, G. K. Smyth, limma powers differential expression analyses for RNA-sequencing and microarray studies. *Nucleic Acids Res* **43**, e47 (2015).
64. B. Phipson, S. Lee, I. J. Majewski, W. S. Alexander, G. K. Smyth, Robust hyperparameter estimation protects against hypervariable genes and improves power to detect differential expression. *Ann Appl Stat* **10**, 946-963 (2016).
65. C. W. Law, Y. Chen, W. Shi, G. K. Smyth, voom: Precision weights unlock linear model analysis tools for RNA-seq read counts. *Genome Biol* **15**, R29 (2014).

66. G. K. Smyth, J. Michaud, H. S. Scott, Use of within-array replicate spots for assessing differential expression in microarray experiments. *Bioinformatics* **21**, 2067-2075 (2005).

AUTHOR MANUSCRIPT

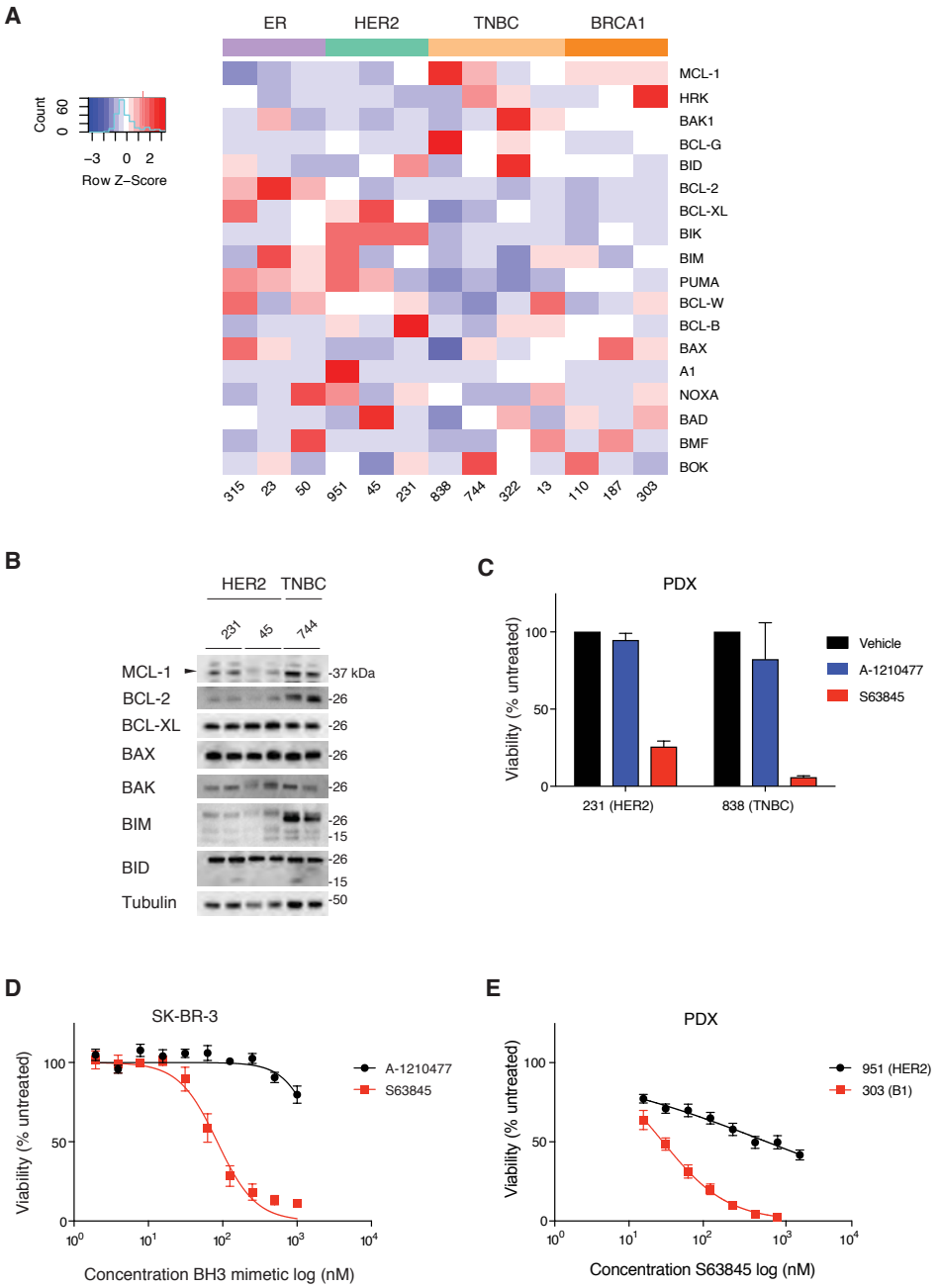

Fig. S1. Expression of BCL-2 family members and sensitivity to S63845 or A-1210477. (**A**) Heat map of mRNA expression of BCL-2 family members obtained from RNAseq data of PDX models (n = 4 for 951T and 322T; n = 2 for the remaining PDX tumors). mRNA expression data are provided in table S2. (**B**) Western blot of BCL-2 family members in PDX tumors 231 and 45 (HER2-amplified) and 744 (TNBC). Tubulin was used as a loading control. (**C**) HER2-amplified PDX 231 and TNBC PDX 838 tumor cells were cultured for 24 hours in mammosphere medium in the presence of S63845 or A-1210477 (at 1 µM), and viability was determined by CellTiter-Glo. Shown are mean ± s.e.m. for n = 3 independent experiments. (**D**) SK-BR-3 cells were treated for 24 hours with increasing concentrations of the MCL-1 inhibitors A-1210477 or S63845 and viability assessed using CellTiter-Glo. Shown are mean ± s.e.m. for 3-5 independent experiments. (**E**) PDX 951 and 303 tumor cells (3 x 10^4 per well) were cultured for 24 hours in mammosphere medium in increasing concentrations of S63845 and viability assessed using CellTiter-Glo. Shown is mean ± s.e.m. for 3 independent experiments. B1, *BRCA1*-mutant tumor.

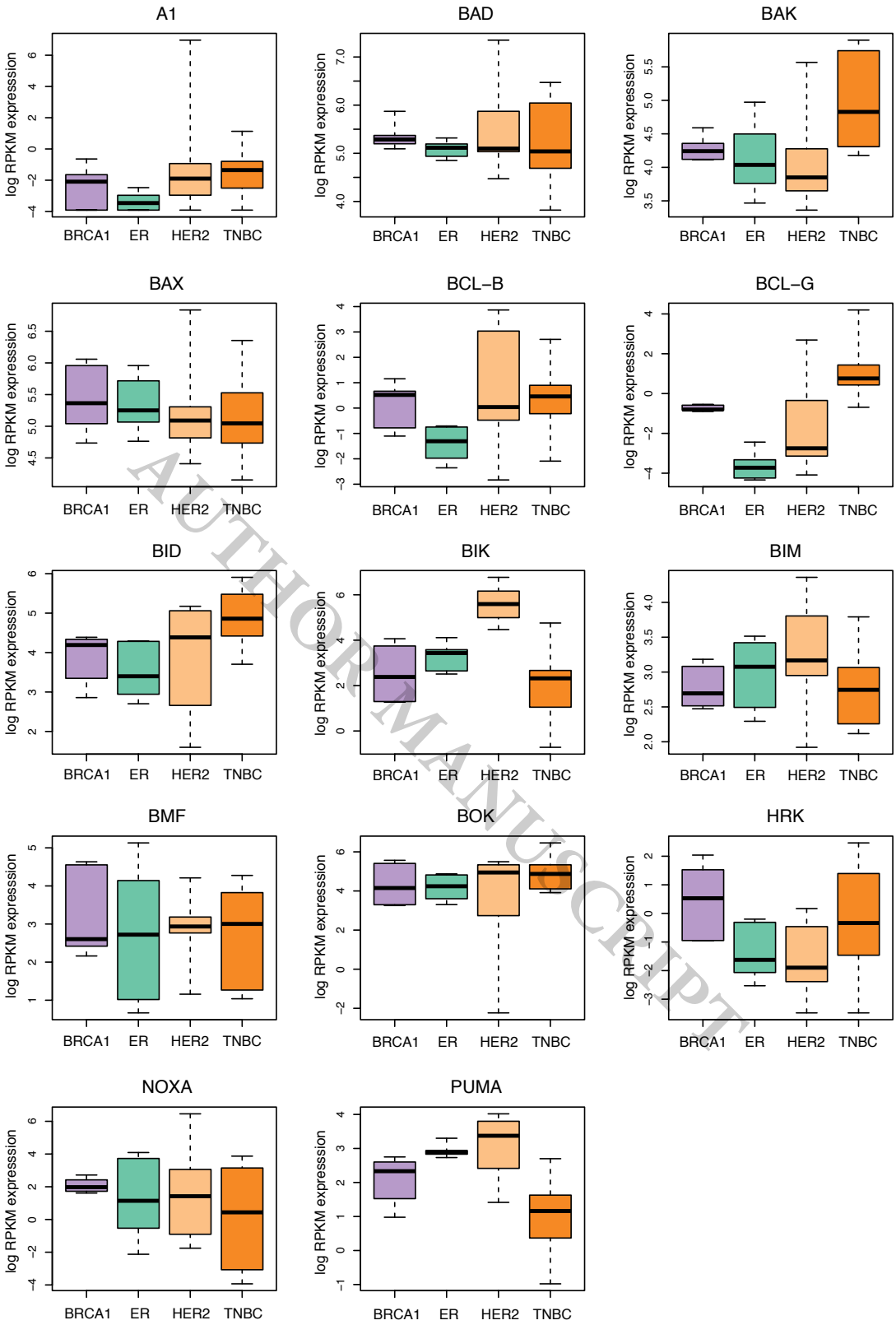

AUTHOR MANUSCRIPT

Fig. S2. RNAseq analysis of BCL-2 family members in PDX models. Box plots representing the expression of BCL-2 family members in PDX models as determined by RNAseq analysis, as described for Fig. 1A. mRNA expression data are provided in table S3.

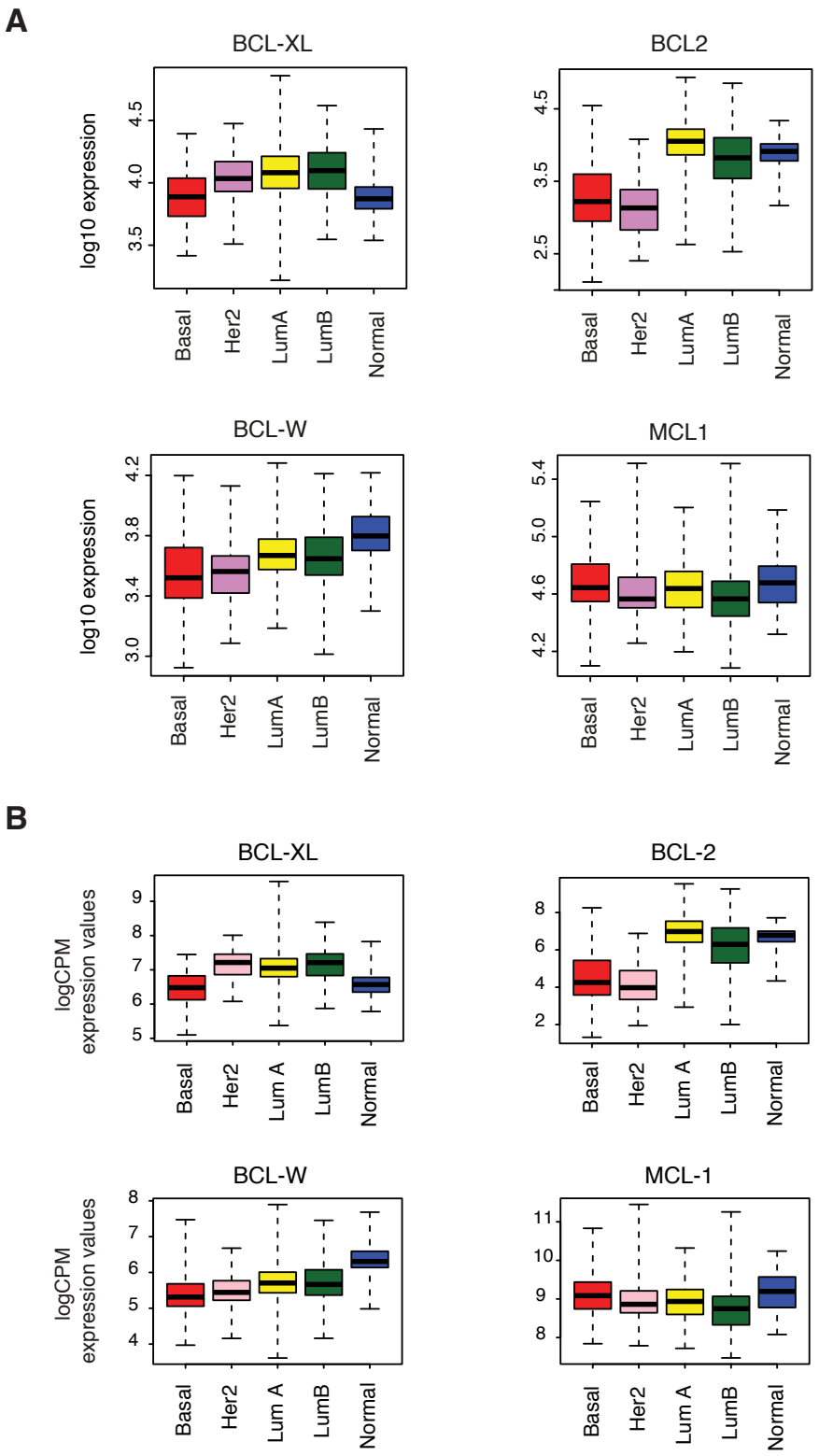

Fig. S3. Expression of *BCL-XL*, *BCL-2*, *BCL-W,* and *MCL-1* in METABRIC and TCGA databases. Box plots representing the expression of *BCL-XL*, *BCL-2*, *BCL-W,* and *MCL-1* from the (**A**) METABRIC (*1*) and (**B**) TCGA (*31*) datasets. Plots show log10 normalized intensities (METABRIC) or log2 counts per million (logCPM; TCGA). mRNA expression data are provided in table S4.

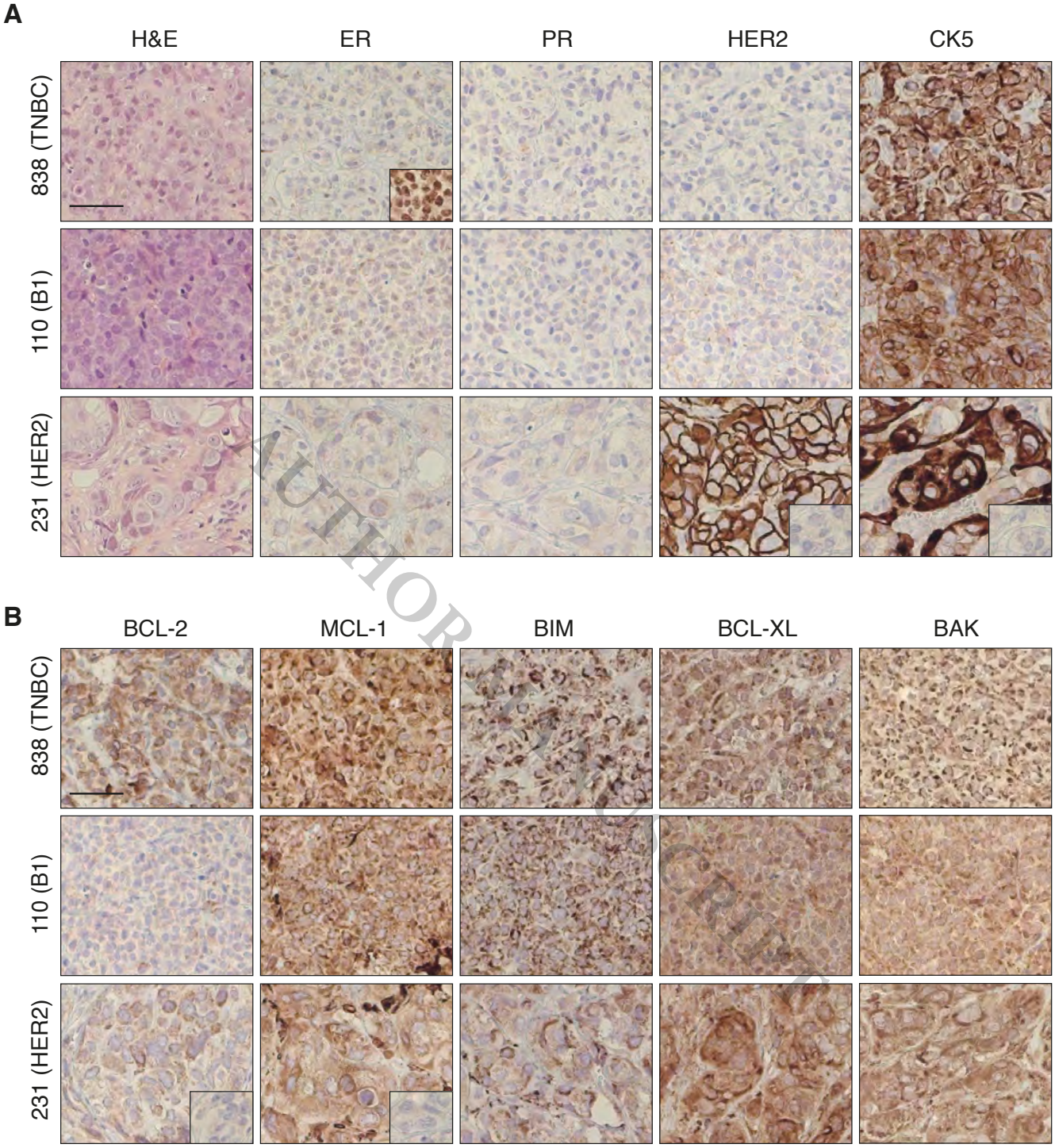

AUTHOR MANUSCRIPT

Fig. S4. Characterization of ER, PR, HER2, and BCL-2 family member protein expression in PDX models by immunohistochemistry. (**A**) Immunostaining of PDX models 838, 110, and 231 for ER, PR, HER2, and cytokeratin 5 (CK5). Insets: PDX 838, ER positive control; PDX 231, isotype controls. Scale bar, 50 µm. (**B**) Immunostaining for BCL-2, MCL-1, BIM, BCL-XL, and BAK. Insets: isotype controls. Scale bar, 50 µm. B1, *BRCA1*-mutant.

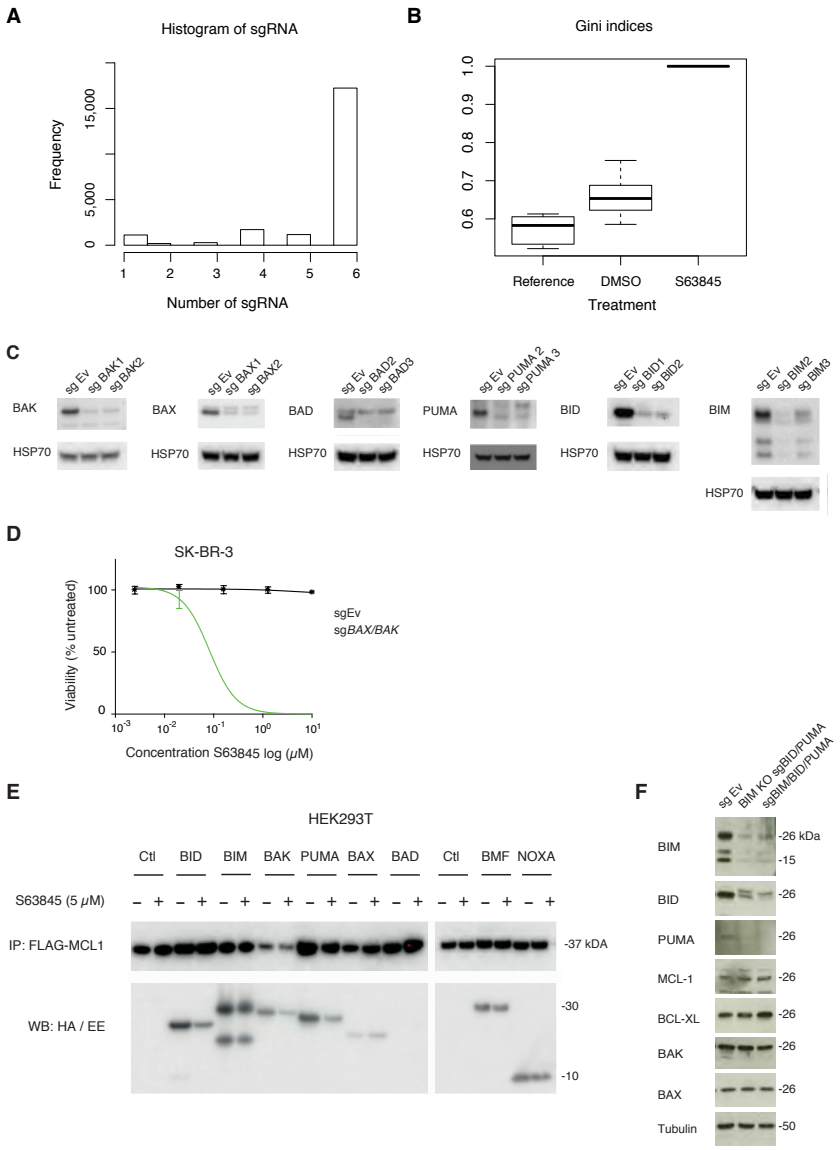

Fig. S5. Deep sequencing of genome-wide lentiviral sgRNA libraries, knockdown of BH3 proteins, and S63845 mediated disruption of MCL-1 complexes containing BH3-only proteins. (**A**) Distribution of the number of sgRNAs per gene detected after the infection of SK-BR-3 cells with the lentiviral library. (**B**) Boxplot of Gini dispersion indices for each treatment. The Gini index for the S63845 treated pool is close to one, showing that a small number of sgRNAs are far more abundant than the rest, while the reference and DMSO treated control samples have lower indices, indicating more even coverage of the sgRNAs. (**C**) Knockdown of BH3 proteins using two CRISPR-Cas9 guides. Western blot showing reduced protein amounts after knockdown of *BAK*, *BAX*, *BAD*, *PUMA*, *BID,* and *BIM*. HSP70 was used as a loading control. (**D**) SK-BR-3 cells infected with CRISPR-Cas9 guides targeting BAK and BAX were treated with increasing concentrations of S63845 for 24 hours and viability assessed using CellTiter-Glo. Shown is mean ± s.e.m. for 3 independent experiments. (**E**) HEK293T cells were transfected with a FLAG-tagged MCL-1 construct and HA-tagged (BID, BIM, BAK, PUMA, BAX, BAD) or EE-tagged (BMF, NOXA) constructs. Cells were treated with or without S63845 (5 μM) before lysis and immunoprecipitation of FLAG-tagged proteins followed by western blotting for HA, EE, and FLAG. For the negative controls (Ctl), no anti-FLAG antibody was used for immunoprecipitation. (**F**) Western blot showing reduced BIM, BID, and PUMA in the Cas9 BIM KO sg*BID/PUMA* and sg*BIM/BID/PUMA* selected clones. Tubulin was used as a loading control.

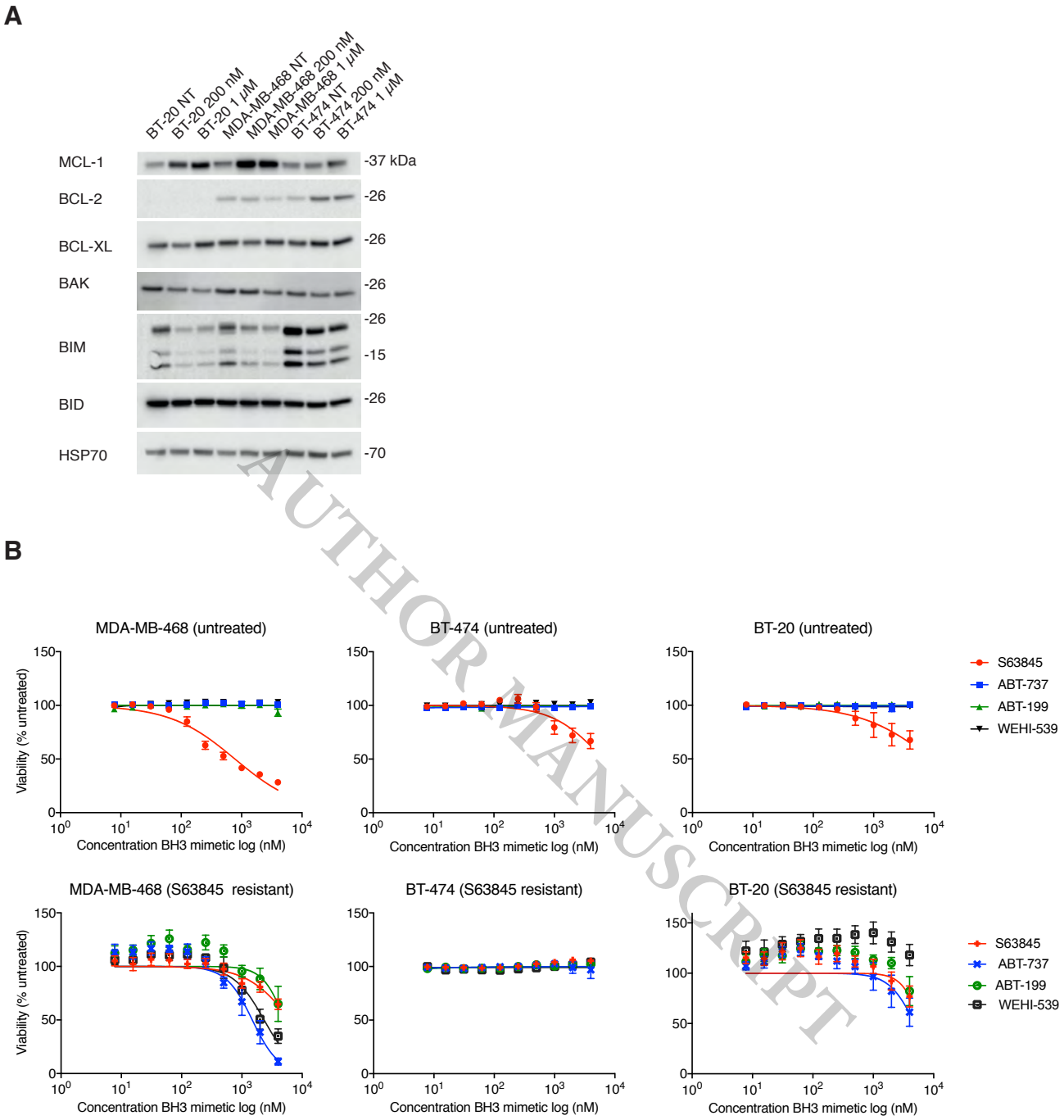

AUTHOR MANUSCRIPT

Fig. S6. Generation and analysis of S63845 resistant cell lines. (**A**) To evaluate the effect of long-term exposure to S63845, BT-20, MDA-MB-468, or BT-474 cells were treated continuously with S63845 (200 nM or 1 μM) or left untreated. Lysates collected at six weeks were subjected to Western blot analysis for MCL-1, BCL-2, BCL-XL, BAK, BIM, and BID. HSP70 was used as a loading control. (**B**) Cells from (**A**) were treated with S63845, ABT-737, ABT-199, or WEHI-539 (1 μM) and viability determined using CellTiter-Glo. Shown are results for untreated cells compared to continuous treatment with 1 μM S63845 (S63845 resistant) for each cell line. Shown is mean ± s.e.m. for 3 independent experiments.

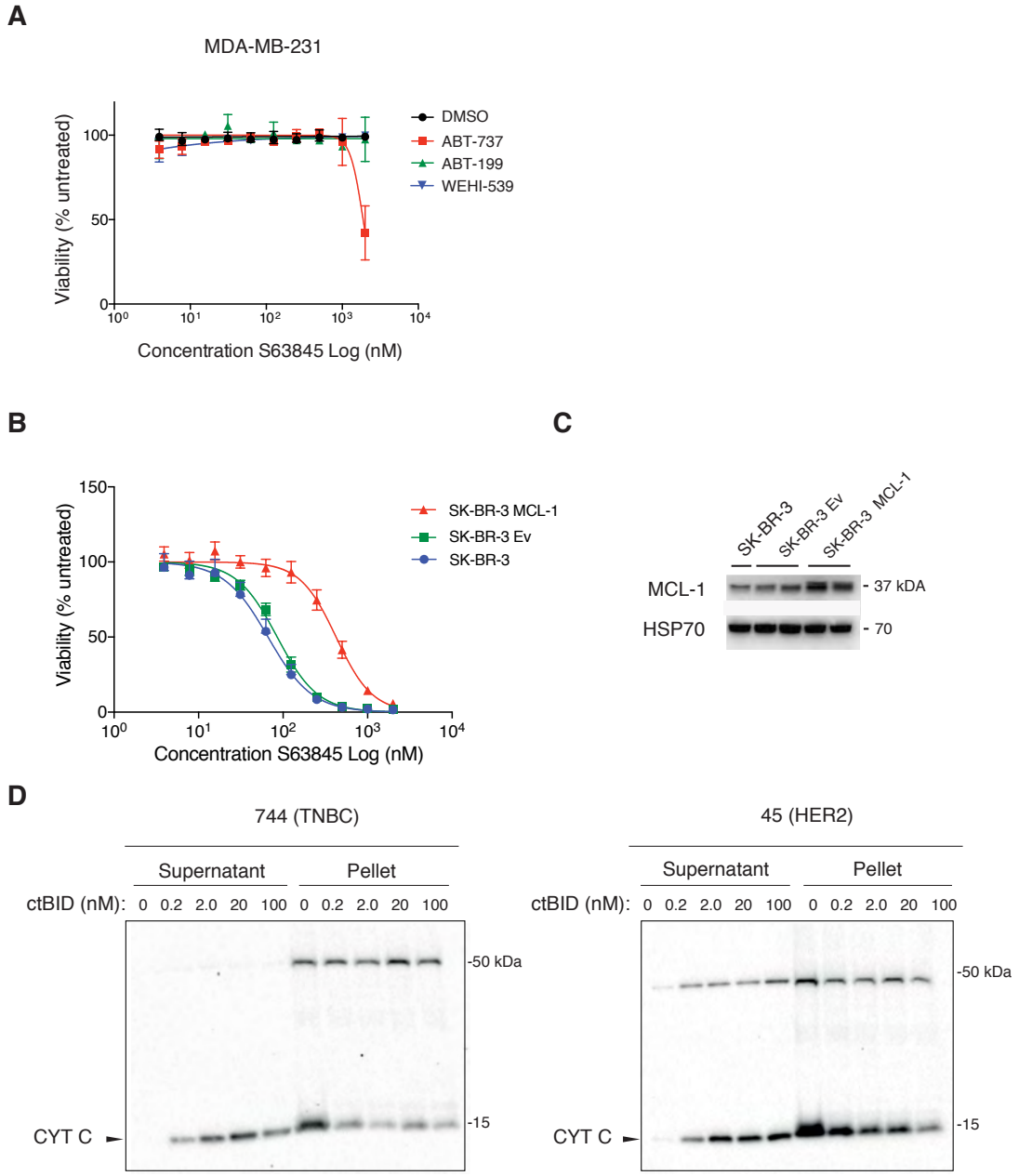

Fig. S7. Exploring molecular mechanisms of resistance to S63845. (**A**) MDA-MB-231 cells were treated with ABT-737, ABT-199 or WEHI-539 (1 μM) and increasing concentrations of S63845 and viability determined compared using CellTiter-Glo. (**B**) MCL-1 was overexpressed in SK-BR-3 cells by retroviral infection and cells treated with increasing concentrations of S63845. Viability was assessed at 24 hours using CellTiter-Glo and compared to native cells and cells infected with empty vector. Shown is mean ± s.e.m. for two biological replicates performed in duplicate. (**C**) Western blot of cell lysates from (**B**) confirming MCL-1 overexpression in the retrovirally infected cells. (**D**) PDX 744 and 45 tumor cells (3 x 10^6 cells for each PDX) were permeabilized with 0.025% digitonin buffer to separate the cytosolic (supernatant) and membrane fraction. The membrane fraction was activated with ctBID at increasing concentrations and incubated at RT for 30 min followed by centrifuging at 13,000 rpm to separate the supernatant and pellet component prior to being run on SDS-reducing gel and probing for cytochrome *c* (CYT C) release.

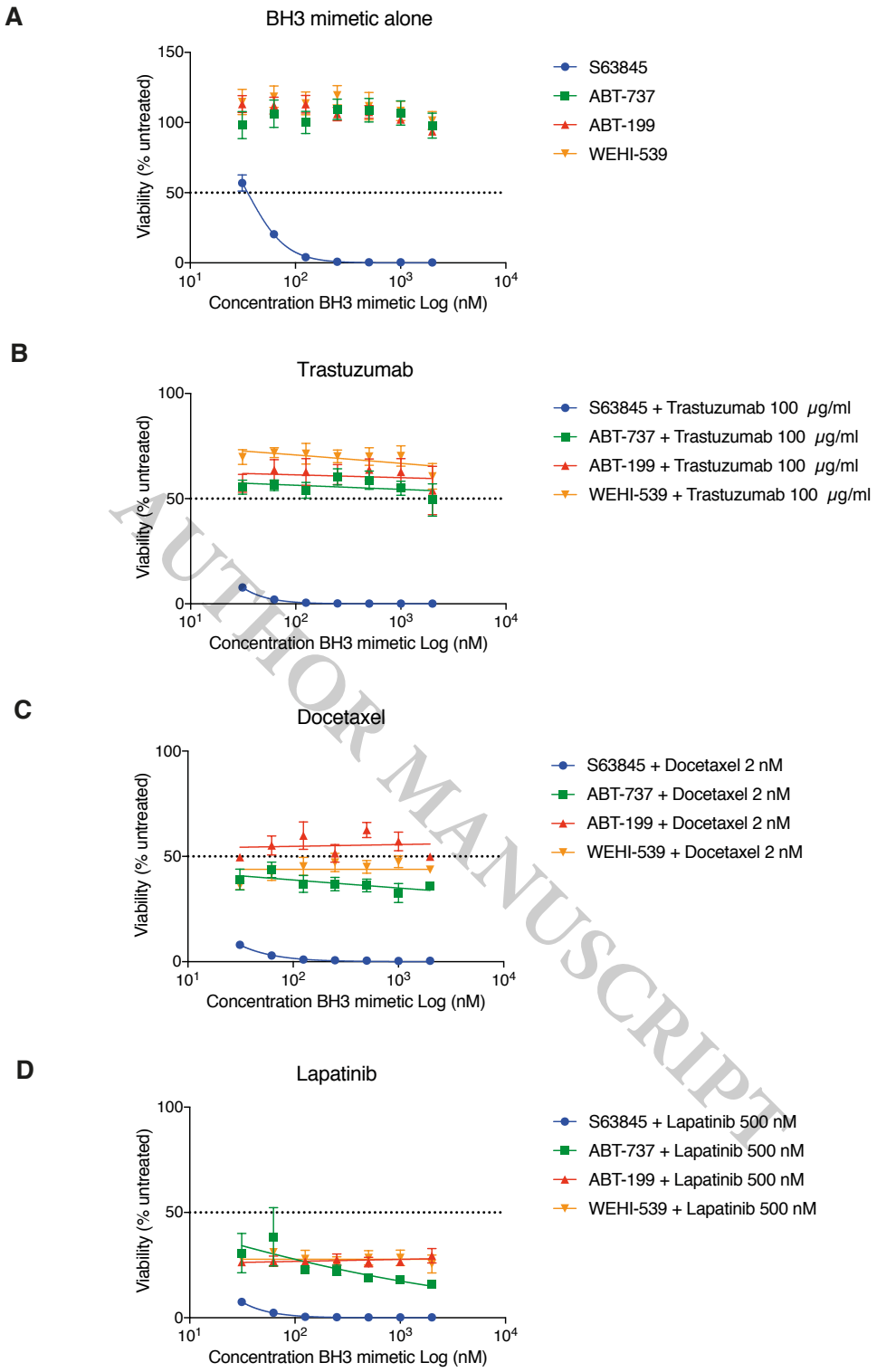

AUTHOR MANUSCRIPT

Fig. S8. Effect of concomitant treatment of SK-BR-3 cells with a BH3 mimetic and trastuzumab, lapatinib or docetaxel. (**A**) SK-BR-3 cells were treated with increasing concentrations of S63845, ABT-737, ABT-199 or WEHI-539, alone or in combination with (**B**) trastuzumab (100 μg/ml) for 96 hours, (**C**) docetaxel 2 nM for 72 hours, or (**D**) lapatinib 500 nM for 72 hours, and viability assessed using CellTiter-Glo. Horizontal dotted lines show 50% viability. Shown is mean ± s.e.m. for 3 independent experiments.

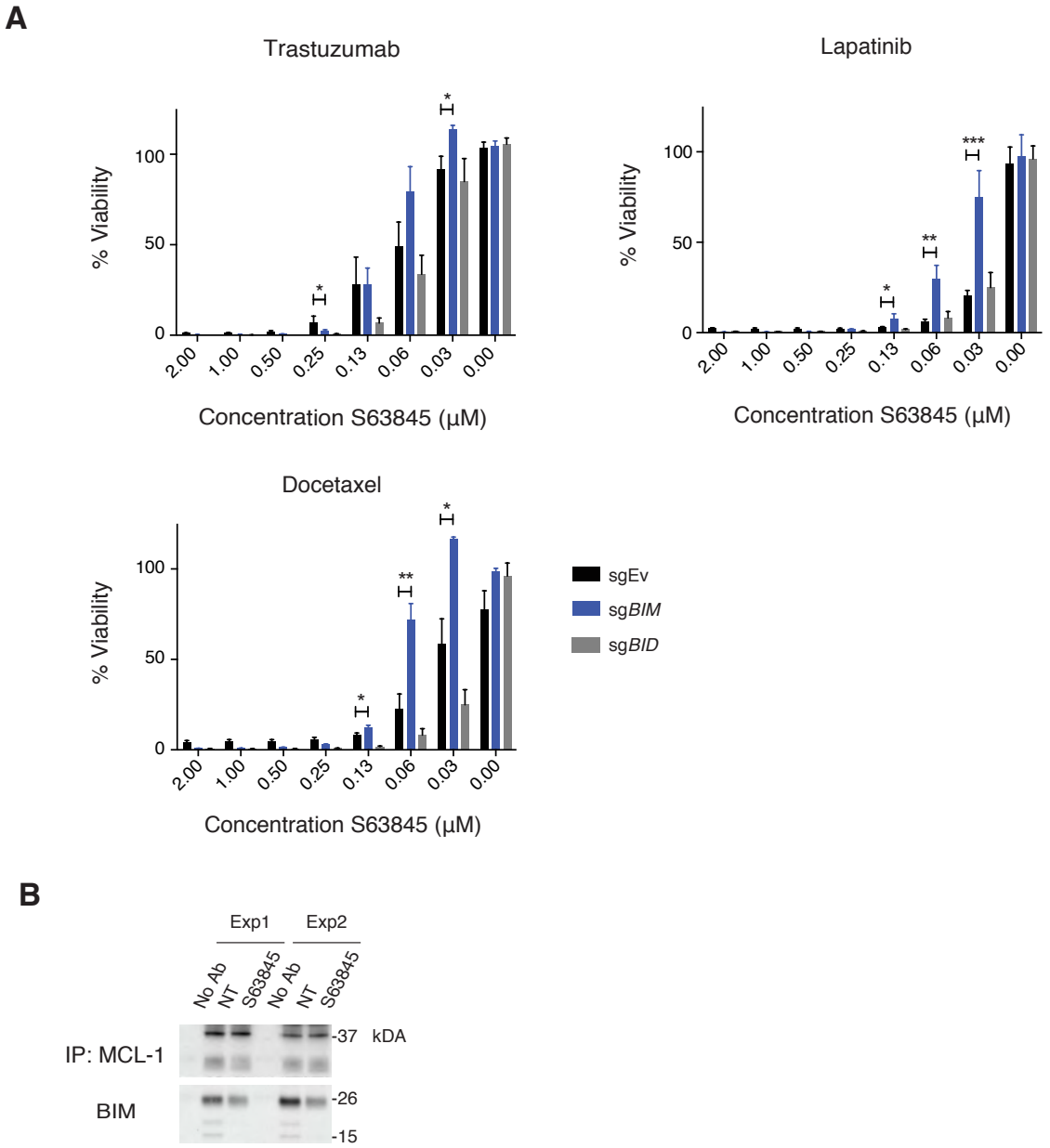

Fig. S9. Role of BIM in the synergistic effect of S63845. (**A**) SK-BR-3 cells infected with CRISPR-Cas9 guides targeting pro-apoptotic protein BIM (sg*BIM*) or BID (sg*BID*) and empty vector (sgEv) control were treated with increasing concentrations of S63845 with trastuzumanb (100 μg/ml), lapatinib (500 nM) or docetaxel (2 nM) for 72 hours and viability assessed using CellTiter-Glo. Shown is the mean ± s.e.m. for 3-5 independent experiments. * $p < 0.05$; ** $p < 0.005$; *** $p < 0.001$. (**B**) Cells from PDX 838 were treated for 5 hours with S63845 (5 μM) before lysis and immunoprecipitation of MCL-1 followed by western blotting for BIM. In the 'No Ab' samples, no MCL-1 antibody was used for immunoprecipitation, as negative control. Results for two independent experiments (Exp 1 and Exp 2) are shown. NT, no treatment.

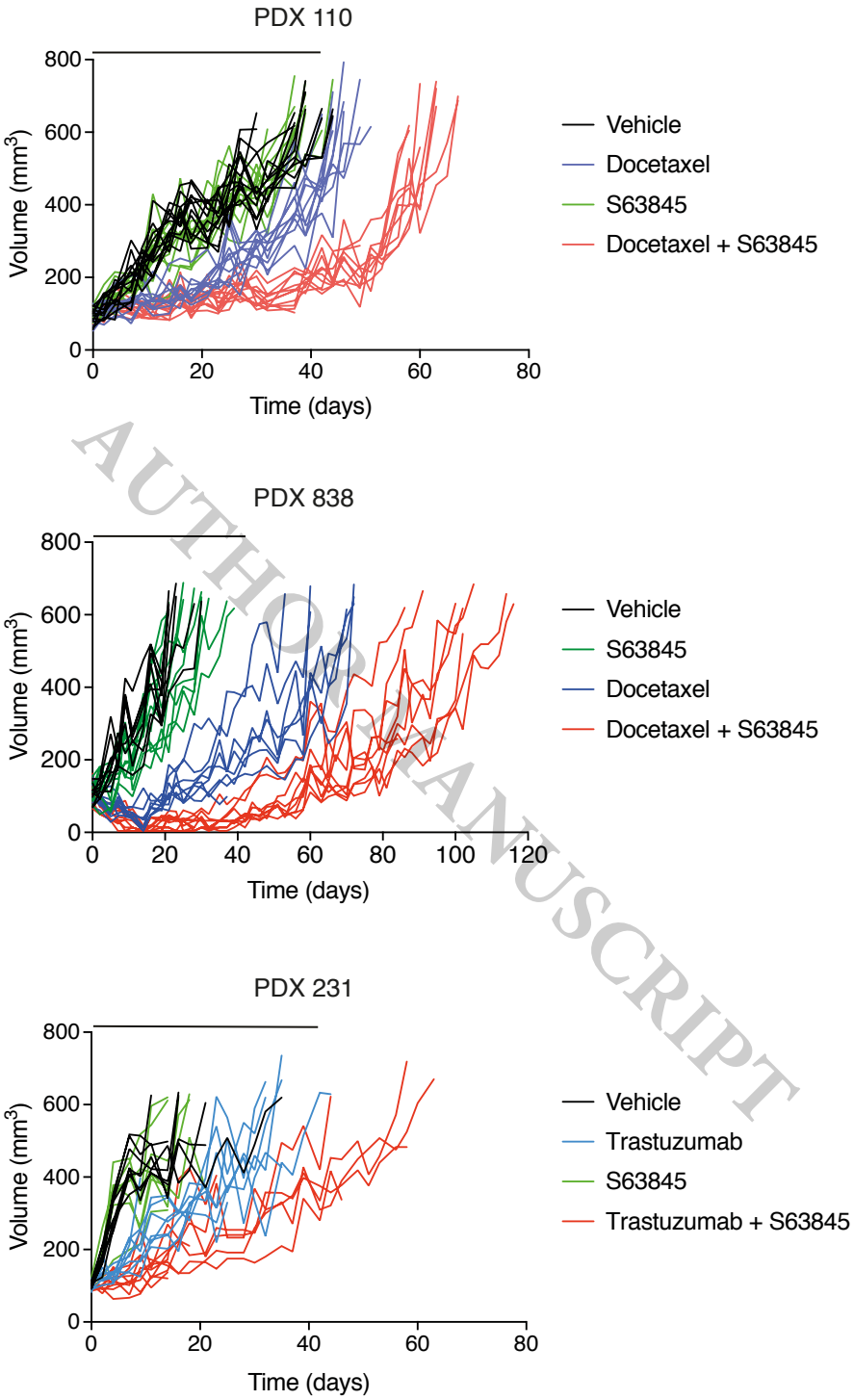

AUTHOR MANUSCRIPT

Fig. S10. **Individual tumor growth curves in TNBC and HER-2 amplified PDXs after combination treatments with S63845 and docetaxel or trastuzumab**. Tumor growth curves for individual mice from PDX models 110, 838, and 231 shown in Fig. 4. The black bars indicate the total duration of treatment.

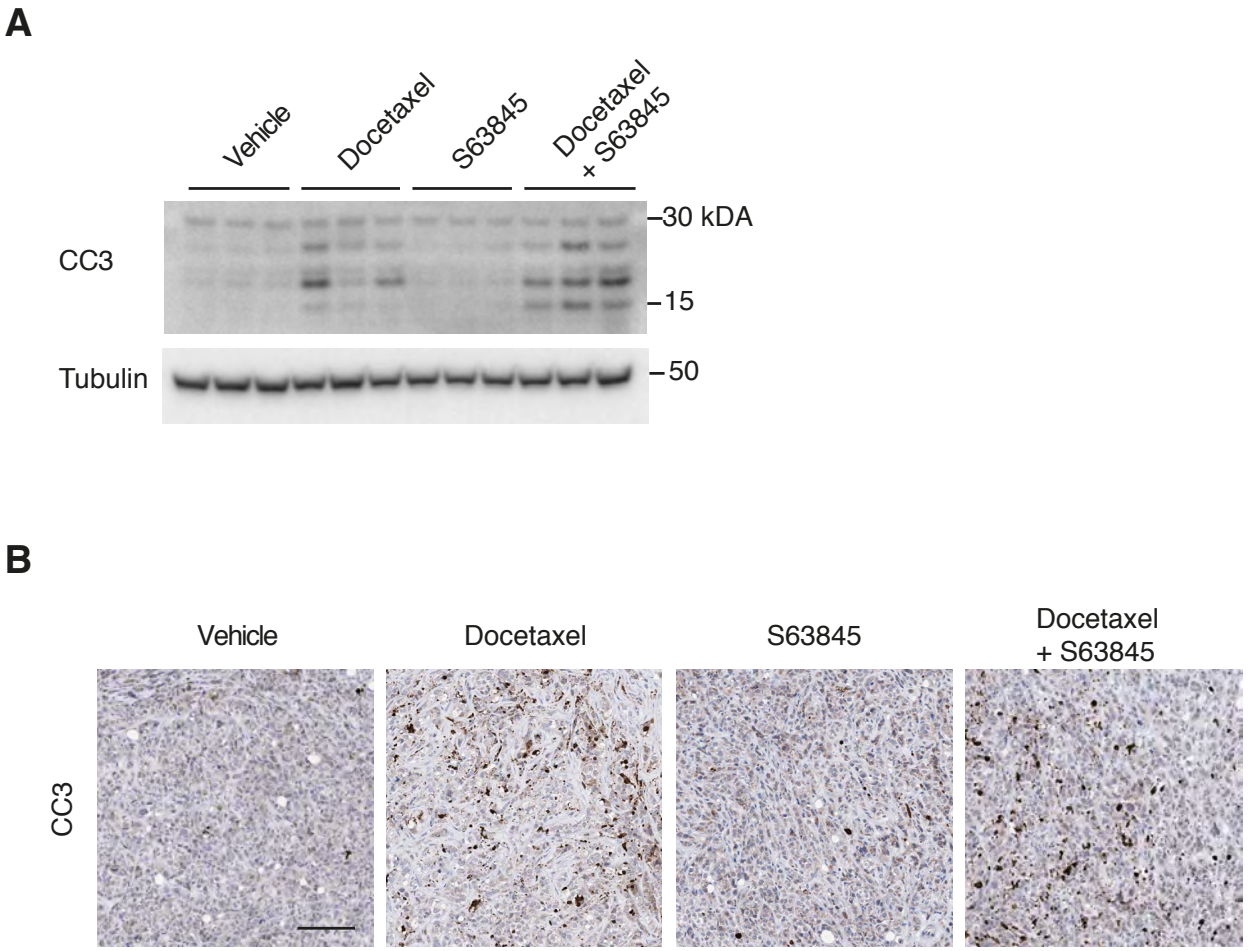

Fig. S11. Effect of combination therapy on tumor cell death. (**A**) Western blot of protein lysates from PDX 838 tumors for cleaved caspase 3 (CC3) after treatment of mice with vehicle, docetaxel (10 mg/kg i.p.) plus vehicle for S63845, S63845 (25 mg/kg i.v.) plus vehicle for docetaxel, or combined docetaxel and S63845. Mice were treated with docetaxel (or vehicle) followed by S63845 (or vehicle) 24 hours later. Tumors were collected 16 hours after the S63845 treatment (n = 3 tumors per treatment arm). Tubulin was used as a loading control. (**B**) Representative tumor sections from (**A**) immunostained for cleaved caspase 3. Scale bar, 100 μm.

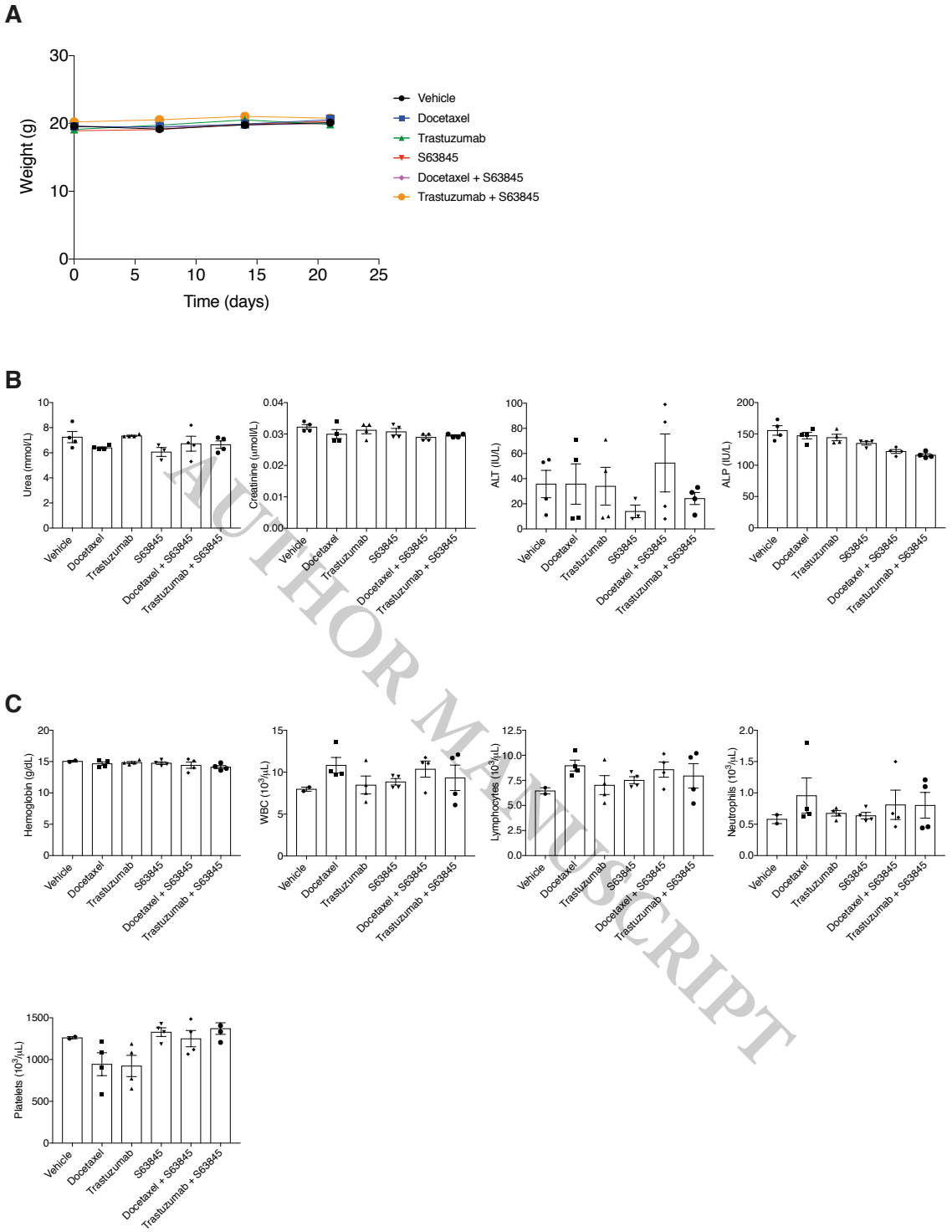

AUTHOR MANUSCRIPT

Fig. S12. Effect of combination therapy on mouse weight, biochemistry, and blood counts. (**A**) For toxicity studies, mice (C57BL/6) were treated with docetaxel (10 mg/kg on day 1), with trastuzumab [once with loading dose of 30 mg/kg on day 1 and with maintenance dose (15 mg/kg) on days 8 and 15], with S63845 (25 mg/kg on days 2, 9, and 16), with docetaxel and S63845, or with trastuzumab and S63845. (**A**) Mouse body weights were determined once a week. (**B** and **C**) Terminal bleeds (cardiac punctures) were taken on day 21, and (**B**) serum urea, creatinine, alanine aminotransferase (ALT), and alkaline phosphatase (ALP) and (**C**) blood counts were measured. WBC, white blood count.

Table S1. Clinical, histopathological, and molecular features of primary breast tumors.

Patient ID	**231**	**951**	**45**	**50**	**315**	**838**	**322**	**744**	**110**	**303**	**187**
Age at diagnosis	52	44	48	46	35	67	35	67	36	32	56
Tumor pathology[1]	(L) 120 mm IDC	(R) 35 mm IDC	(R) 22 mm IDC	(L) 75 mm Poorly differentia-ted	(R) 30 mm IDC 20 mm satellite lesion	(R) 37 mm Poorly differentia-ted IDC	(L) 20 mm IDC	(L) 32 mm IDC of pseudo-medullary type	(L) 9 mm infiltrating carcinoma	(L) 35 mm multi-focal IDC	(R) 18 mm + (L) 8 mm IDC
BRE Grade	3	3	3	3	3	3	3	3	2	3	3
LVI[2]	+	–	+	+	–	+	–	+	–	–	R+L: –
Axillary LN[3]	7/16	2/32	1/29	19/20	16/27	7/27	0/1	0/1	0/2	1/1	Not shown
Immuno-histochemistry:											
ER[4]	0% –	<1% –	0% –	40% ++	10-30 % ++	0% –	0% –	0% –	0% –	0% –	0% –
PR[4]	0% -	0% -	40% +	20% ++	10% ++	0% –	0% –	0% –	0% –	0% –	0% –
HER2	3+	3+	3+	2+	–	–	–	equivocal	1+	–	1+
CISH/SISH	14.9	21.9	20.5	2.0	n.d.	n.d.	n.d.	1.8	n.d.	n.d.	2.0
Tumor genotype: *BRCA1*									c.181T>C (pCys61Arg)	c.5467G>A in exon 23	3875_3878 del GTCT (STOP 1282)
MCL-1 amplification	–	–	–	–	–	–	–	–	–	–	–

n.d. not done.
[1] IDC, invasive ductal carcinoma.
[2] LVI, lymphovascular invasion.
[3] LN, lymph node.
[4] ER and PR expression: reported per cent of positive tumor cells; – neg, + weak, ++ mod.